WATERTOWN ARSENAL, WATERTOWN 72, MASS.

WATERTOWN ARSENAL LABORATORY

EXPERIMENTAL REPORT

NO. WAL. 111/7-4

[illegible]PE OF THE NECK AND THE FRACTURE OF TENSION SPECIMENS.

BY

P. W. Bridgman
Harvard University

DATE 28 January 1944

WATERTOWN ARSENAL
WATERTOWN, MASS.

DISCLAIMER NOTICE

PB 4069

(14)

Watertown Arsenal Laboratory
Report Number WAL-111/7-4
Purchase Order No. 3-13782

(11) 28 January 1944

PLASTIC PROPERTIES OF STEEL

(6) The Shape of the Neck and the Fracture of Tension Specimens.

FOREWORD

(12) 87

The tensile test has been used, and is still being used, as the standard test for investigating the plastic properties of metals. The interpretation of the data taken beyond necking has been somewhat ambiguous due to the presence of transverse stresses of unknown magnitude. Professor Bridgman has removed this ambiguity by the calculation, presented in this report, of the three dimensional stress system in the neck of a tensile specimen. He also presents further observations upon the nature of and the conditions for fracture.

(9) Experimental rept.,

C. Zener
Senior Physicist

APPROVED:

(10) P. B. Bridgman

H. H. ZORNIG
Colonel, Ordnance Dept.
Director of Laboratory

code 23
cp

370850

50B

The Shape of the Neck and the Fracture of Tension Specimens.

SUMMARY

The following general results have been found for necking and fracture in tensile tests.

The ratio of the radius of the neck to the radius of curvature of the contour of the neck at minimum cross section increases continuously with increasing strain but at a decreasing rate from a value zero at the inception of necking to a value of the order of 2 at natural strains of 4, the highest reached in this work. This ratio is a function primarily of strain (Fig. 4), and is nearly independent of the material.

With the inception of necking the stress at the minimum cross section changes from a uniform tension to a system in which a hydrostatic tension is superposed upon a uniform tensile stress. The hydrostatic tension increases from zero at the surface to a maximum at the axis. The ratio of the hydrostatic tension to the uniform tensile stress is a function only of the ratio of the radius of the neck to the radius of curvature of the contour. Since the latter ratio is primarily a function only of the strain, the former ratio is also (Fig. 5).

As the strain at fracture is increased by an increase in applied hydrostatic pressure, the area of

the tensile failure in the cup diminishes and disappears at pressures of the order of 200,000 to 300,000 psi. Thereafter the entire failure is by shear (Figs. 15-20). The change in character of the fracture appears to be a legitimate pressure effect and is not an incidental result of the geometry (great necking) accompanying fracture under pressure. The natural strain at fracture is established to be approximately a linear function of the hydrostatic pressure in the medium in which fracture is produced up to pressures of approximately 400,000 psi, twice the range in which the linear relationship has been previously established. The linear relation appears to continue to hold without important modification when pressure passes through the value at which the tensile fracture disappears.

Fracture occurs under the conditions of these tests when the mean of the principal stresses reaches a critical value. This critical value is unchanged by a change in an externally applied hydrostatic pressure or by a change in the contour of the neck by machining. If it is assumed that fracture occurs at a critical mean stress, that the strain hardening curve is linear, and that the relation between hydrostatic pressure and strain at fracture is linear, the ratio of radius of the cross section to the radius of curvature of the contour is determined as a function of the strain. The ratio determined in this way agrees approximately with the experimental values. The mean stress criterion for fracture fixes the pure hydrostatic tension at which fracture occurs without strain ("cohesive strength"). This turns out to be smaller than usually supposed.

RESULTS AND DISCUSSION

This report is divided into two parts: in the first a general investigation is made of the variation of the shape of a tension specimen in the neighborhood of the neck, and in the second a beginning is made of a general investigation of the subject of fracture. The two parts play into each other, because the actual stresses in a tension specimen at the moment of fracture are not given directly by the measured loads, but must be obtained by calculation, and the shape of the neck is an important factor in this calculation. As in previous reports, a particular feature of the experiments has been the covering of a wide range of strain by utilizing the effect of high hydrostatic pressure in increasing ductility.

Part I. The Shape of the Neck of Tension Specimens.

The stress in the neck of a tension specimen is not uniform across the section. In a specimen pulled under ordinary conditions at atmospheric pressure the stress consists of a longitudinal stress uniform across the section with a superposed hydrostatic tension (three equal positive components of principal stress) which varies from zero at the outside surface to a maximum on the axis. Proper consideration of the effect of stress distribution materially modifies the simple picture which is obtained when the average longitudinal stress is considered to be the only stress component. The modification affects both flow phenomena and fracture phenomena. With regard to flow, the significant flow stress is that which prevails at the outer surface of the neck where the stress reduces to a single longitudinal component; this longitudinal component is less than the average longitudinal stress across the neck, so that the effect of recognizing the stress distribution in constructing a curve of flow stress versus strain will be to lower the curve. The factor by which the points on the flow or strain-hardening curve are to be lowered is a function of the shape of the neck, that is, of the ratio of the radius of the cross section of the neck to the radius of curvature of the contour of the neck (a/R in Figure 1). The average stress must be divided by* $(1 + 2 \frac{R}{a}) \log_e (1 + \frac{1}{2} \frac{a}{R})$ to get the corrected flow stress. For average grades of steel this means, to give a single example, that if necking corresponds to a reduction of area of 67 per cent, the corrected flow stress will be approximately 0.8 of the average longitudinal stress. With regard to phenomena of fracture the effect of taking account of stress distribution is even more important.

*P. W. Bridgman: "Stress Distribution at the Neck of a Tension Specimen". ASM Preprint, 1943.

Fracture in a tension specimen starts on the axis, where the mean hydrostatic tension (one third the sum of the three principal stress components) is a maximum and where the brittleness produced by the hydrostatic pressure is therefore also a maximum. Fracture involves the entire stress system, and in reporting the results of a fracture both the longitudinal and transverse components on the axis should be given. On the axis the transverse components are equal to $\log_e (1 + \frac{1}{2} \frac{a}{R})$ times the flow stress. In the example above, where the reduction of area was 67 per cent, the transverse component of stress on the axis is approximately 0.4 of the average longitudinal stress.

A complete report of the results of a flow or fracture experiment for strains greater than that which corresponds to the beginning of necking demands, therefore, that the shape of the neck, or the ratio a/R, be determined in addition to the average longitudinal stress. The importance of knowing this ratio is greater the greater the reduction of area. A complete theory of the plastic flow in a tension specimen should give a/R in terms of the strain hardening data for any degree of necking. One would perhaps expect in general that for a given degree of necking a/R should be greater the greater the slope of the strain-hardening curve. However, if one attempts to work out a theory on this basis one encounters difficulties. One may seek for a connection between the increase of cross section as one moves away from the neck and the corresponding change of strain, but on working out the details it will be found that the first derivative of the strain vanishes at the neck, so that the condition will have to be a condition on the second derivative of the strain. Any such condition would appear not likely to lead to a sharp condition on the first derivative or slope of the strain-hardening curve, and one might even draw the conclusion that the slope of the strain-hardening curve cannot greatly affect the shape of the contour. However this may be, the mathematical solution has not yet been obtained that gives a/R in terms of other measurable quantities, and the subject has to be treated on an empirical basis.

The experimental problem is to find a/R as a function of strain at the neck for a number of steels of varying compositions and with different strain-hardening curves. If it should fortunately prove that a/R is not sensitive to the kind of steel or the slope of the strain-hardening curve, then the same correction for stress distribution could be made for all steels at the same reduction of area, and it would not be necessary to make a special determination of a/R in addition to the conventional reduction of area for each tensile test. In any event it is to be anticipated that certain experimental regularities will be found so that for any particular grade of steel the correction for stress distribution could be made by referring to a previous experiment on a similar steel.

A large mass of experimental material is now at hand bearing on this question; this includes former experiments in which the relevant data were collected only incidentally and which have not yet been reported in detail, and new experiments made for this particular purpose. In general a number of specimens should be examined for any one grade of steel to avoid error from scattering of the individual points. Most of the former measurements not directed to this explicit purpose suffer from the disadvantage that only two points were determined for any particular grade of steel, and this is not sufficient.

In order to obtain a wide range of strain without fracture the tension specimens were pulled, as usual, in a medium under hydrostatic pressure. The pressure might range as high as 400,000 psi; the precise value of the pressure might vary somewhat with the desired amount of strain. The precise details are unimportant, since previous work has shown that flow phenomena are little affected by hydrostatic pressure; this is confirmed by the fact that in the present work no correlation could be found between pressure and a/R. Measurements of stress versus strain under pressure were made according to the regular routine, so that data are at hand for the complete stress-strain curves; however it is only the maximum points on the curves that are used here. After termination of the pressure part of the experiment, the dimensions of the specimen were measured at atmospheric pressure. If the amount of necking was only slight, the radius of curvature of the contour was obtained by calculation from measurements of the diameter at points spaced along the axis at 0.05 cm intervals symmetrically on both sides of the neck. If the radius of curvature was smaller, so that the outline was not appreciably circular over a distance of at least one millimeter, the radius was determined in a special appliance by which a long tapered conical pin was rested on the contour and slid back and forth until the contact with the neck appeared best to the eye, after which the diameter of the cone at the place of contact was measured.

If it is desired to obtain a connection between strain-hardening and a/R, then the reduction of area under the tensile load must not be pushed beyond the point where the accuracy of the stress determination is materially reduced because of reduction of the total tensile load. If, however, the interest is in a/R as a function of strain, necking can advantageously be pushed considerably further, because now the necessary measurements are purely geometrical and can be made with the requisite accuracy. Even here, however, there is a limit to the reduction of area compatible with significant results. When the reduction is pushed to an extreme, geometrical irregularities become prominent: the section of the neck is no longer circular, the radius of curvature of the contour varies with azimuth about the longitudinal axis, the exterior surface at the narrowest part of the neck becomes rough and coarsely granular in structure, and, in some grades of steel in particular, longitudinal folds and ridges make their appearance. The latter effect, longitudinal folds and ridges, is probably associated with the presence of small scale inhomogeneities or dirt in the steel, but the other effects are shown by all steels and are probably associated with finite grain size. Much the same sort of thing has been round in studying the collapse of hollow cylinders in the fourth report; if collapse is pushed too far the original circular figure is lost and the cavity becomes polygonal in outline, different edges of the polygon being contributed by different grains. In the steels studied here geometrical irregularities become uncomfortably prominent at natural strains greater than about 4, that is, for extensions greater than 50 or 60 fold. For other metals, in particular copper and aluminum, geometrical irregularities become prohibitive at smaller strains. Thus a particular specimen of commercial aluminum, when pulled to an extension of 15 fold, exhibited a neck diameter 35 per cent greater at the maximum than at the minimum and a contour which in one azimuth had a sharply reëntrant angle (zero radius of curvature) and in another azimuth was flat for a length of the order of magnitude of the radius (infinite radius of curvature).

Three special steels were investigated in the present work. These were commercial annealed bar stock 5/8 to 1/2 inch in diameter of SAE specifications 1315 (manganese steel), 2320 (nickel steel), and 4140 (chromium steel). The Rockwell C hardnesses of these were respectively: 21.1, 29.1, and 34.5. Four specimens of each of these were measured in the strain range up to 2.5, not too high to give good values for the flow stress. In addition, and primarily for other purposes described in the second part of this report, measurements were made on four different heat treatments of a 1045 steel. For two of these heat treatments a/R was determined for only two specimens, but enough measurements were made on the two other treatments to be significant; these are the A5 and A6 series described in detail in the second part of this report. The numerical results of the measurements for the three special steels are given in Table I and those for the A5 and A6 series in Tables III and IV in the second part. The results are shown graphically in Figures 2 and 3; in Figure 2 a/R is given as a function of the natural strain, and in Figure 3 the flow stress, corrected for stress distribution as already outlined. The individual points for the three SAE steels show an unusual degree of regularity in both figures. Furthermore, the a/R points for these three steels all lie on a single curve within the limits of error, in spite of the fact that the strain-hardening curves of these steels, as shown in Figure 3 have different heights and somewhat different slopes. The points for the two 1045 steels for some reason are much less regular; however, there would seem to be little doubt that the a/R points for them lie appreciably below the curve for the three SAE steels, whereas their strain-hardening curves lie little if any below that of the lowest of the SAE steels. There would appear therefore to be a variation in a/R beyond the limit of experimental error, but this variation does not appear to be correlated with the strain-hardening curve. In order to exhibit the effect of a still wider variation in the strain-hardening curve, the points for the heat treatment of the 1045 steel which gave the highest lying strain-hardening curve, the A7 series, are also given in Figures 2 and 3, although only two specimens were measured. The stress-strain curve of this heat treatment is markedly higher than the highest of the SAE steels, and its slope is also greater, but the a/R points lie on the same curve.

In Figure 4 all the observed values of a/R measured in my experiments to date are plotted against strain. Most of the points are plotted indiscriminately, without attempting to group the points obtained from the same grades of steel. Included are all the values for different heat treatments of 1045 steel investigated for the Arsenal both in this and previous reports, values for a number of different compositions of armor plate determined in connection with a contract with the N.D.R.C., and several points for materials different enough from the average to demand separate designation, as shown in the rubric in Figure 4. This includes the points for a soft 1020 steel determined for the Arsenal, and special measurements of my own on brass, a bearing bronze, and "Ketos" steel treated to a Rockwell C of 52.5 and with a stress-strain curve lying much higher than that of any of the other steels.

Examination of Figure 4 shows that there is no consistent variation of a/R with the properties of the material large enough to attempt to take into account for general purposes, and the points may be represented by an average curve. By the use of the average curve it should be possible to describe the stress distribution for any steel with a fair approximation, given only the natural strain. That is, for most purposes a special measurement of the radius of curvature of the contour of the neck may be dispensed with. We may illustrate the magnitude of the possible error by supposing a case representing the extreme divergence of any of the points shown in Figure 4. Thus consider a steel stretched to a natural strain of 3 with a mean longitudinal stress (tensile load divided by the neck area) of 200,000 psi, and suppose that the actual value of a/R for this specimen is that which is normally, that is according to the curve, associated with a strain of only 2. Then the flow stress for this specimen, calculated by using the curve, would be 147,000 psi against a correct flow stress of 155,000 psi, and the hydrostatic tension on the axis arising from necking calculated by using the curve would be 95,000 psi against a correct value of 83,000 psi.

It should be remarked, however, if use is made of these results under conditions wider than those covered in these reports, that all the specimens included in Figure 4, with two exceptions, had an initial ratio of length to diameter somewhere in the neighborhood of 3. It is conceivable that this ratio may have some effect on a/R, and this possibility should be kept in mind. It is probable, however, that any such effect would be most noticeable at small strains and that at large strains any initial effect would be wiped out by the large distortion. In an attempt to throw experimental light on this question two specimens are made with twice the usual ratio of length to diameter; wider variation was not feasible within the limitations of the present apparatus. The results for these two specimens are shown by the accented points in Figure 4. It would appear that any effect of ratio of initial length to diameter is not large, but the number of observations is too small to justify any more definite conclusion.

Assuming a universal relation between a/R and natural strain for all materials, it is possible to make a table giving the effect of stress distribution, that is, to give the factors by which the average longitudinal stress across the neck must be multiplied to give the flow stress at the outer surface (where there is no other stress component under normal conditions), and the hydrostatic tension arising from necking on the axis, where rupture begins. Table II gives the numerical results, and Figure 5 shows them as curves. The values are slightly different from those which were first obtained on the basis of fewer data and which were used in the third report, for example, and correspond to an a/R versus strain curve lying somewhat lower than the curve first used.

Part II. The Effect of Hydrostatic Pressure on Tensile Fracture.

Not only does hydrostatic pressure alter the longitudinal stress component associated with the fracture of a tension specimen but it alters the character of the fracture. The object of the present investigation was to throw further light on the problem of fracture by studying fracture over a wide range of hydrostatic pressures, this permitting a continuous variation in the character of the fracture. It has already been established that the character of the fracture of a steel which normally exhibits a cup-cone break changes with increasing pressure in such a way that the tensile part of the fracture disappears at pressures in the neighborhood of 200,000 psi and above this the fracture is entirely shearing. One specific problem for the present investigation was to find whether there are other observable discontinuities accompanying the change in the character of the fracture; in particular is there a change in the slope of the curve which plots the strain at fracture against the hydrostatic pressure at fracture on passing through the critical pressure 200,000? Another question was whether the change in the character of the fracture is a pure pressure effect or whether it is an incidental effect of the geometry, fracture with increasing pressure taking place with a progressive increase in a/R. It is conceivable that the change in the character of the fracture may be associated with a critical value of a/R.

In studying fracture, tests were made on four different heat treatments of a 1045 steel. The original bar was cut to 14 inch lengths for heat treatment, and all pieces of the same nominal treatment treated together in the same heat of the furnace. The specimens are designated as follows. The first two symbols designate the heat treatment:

A5, quenched into salt at 1100° F from 1575°.
Rockwell B 85.5.

A6, quenched into salt at 800° from 1575°.
Rockwell B 91.7.

A7, quenched into water from 1575° and drawn at 800°.
Rockwell C, 40.3.

A8, quenched into water from 1575° and drawn at 1100°.
Rockwell C, 21.0.

The next symbol, a letter after a dash, denotes from which one of the 14 inch lengths the specimen was cut. There were five lengths in the batches A5 and A6 and hence letters A, B, C, D, E, but only two lengths in batches A7 and A8. The final figure in the designation shows the position in the short length. Thus the specimen designated A5-C1 is the first specimen cut from length C of the batch which was quenched into salt at 1100° from 1575°. All the lengths of treatments A5 and A6 were cut from the same original bar. Due to an accident in the treatment, the batch intended for A7 was lost. The damaged batch was replaced by two lengths from another bar, ostensibly of the same composition.

The program was to first establish the stress-strain curve for each treatment by pulling several samples by an appropriate amount short of fracture, and then to fracture a number of specimens at various pressures spaced over the entire range. The details of the apparatus and method were the same as in previous reports and need not be described further here. Most of the fractures below 200,000 were made in a second apparatus, not hitherto used in the work for the Arsenal. This apparatus has been previously used for extensive work for the N.D.R.C. and is practically identical with the other.

In addition to the measurements of the various forces and the measurements of a/R of the unfractured specimens described in the first part of this report, measurements were made of the area of the tensile part of the fracture of the fractured specimens (area of the bottom of the cup), and the ratios of this area to the total neck area are tabulated. The methods of measuring the fracture have been described in detail in a recent N.D.R.C. report.

The numerical results are given in Tables III, IV, V, and VI. Several cases will be noticed in which no values are given for the various fracture stresses; these are cases in which the reduction of area was so great as to seriously diminish the accuracy of measurement of the tensile load. The reduction of area, however, could be measured with sufficient accuracy in most of even these cases. The "corrected flow stress" of column 7 is obtained from the "uncorrected flow stress" of column 6 (which is merely the tensile load divided by the actual area) by multiplying by the factor described in the first part of this report. In those cases in which a/R was directly measured the factor used was the theoretical factor $\frac{1}{(1 + 2\frac{R}{a})\log_e(1 + \frac{1}{2}\frac{a}{R})}$ as listed in the third column of Table II. If the value of a/R was not directly measured the corresponding factor was taken from the curve of Figure 5 in terms of the known strain at fracture. Column 8, the hydrostatic tension on the axis arising from necking, is obtained by multiplying column 6 by the factor $\frac{1}{1 + 2\frac{R}{a}}$ in those cases where a/R was directly measured, or in other cases by the factor listed in column 4 of Table II or given graphically in Figure 5. The "stress components at fracture" in columns 9, 10, and 11 are the "total stresses" on the axis, the resultant of the hydrostatic pressure of column 2, the flow stress of column 7, and the hydrostatic tension produced by necking of column 8. In particular, $\widehat{rr}$ and $\widehat{\theta\theta}$, columns 9 and 10, are column 8 minus column 2; $\widehat{zz}$, column 11, is column 7 plus column 9 or 10. Column 12, the mean equivalent hydrostatic tension, is one third the sum of columns 9, 10, and 11.

In Table VII are collected various data concerned with specimens dealt with in previous reports but for which all the data were not then given, since they were not pertinent to the purposes of those reports. In particular, the values of a/R were not given, nor the ratio of area of tensile break to total neck area. In addition, the corrected flow stresses at fracture are slightly modified in most cases in comparison with those given in previous reports because of the use of the improved average curve for a/R as a function of strain. The series AII, AIII, AIV has not previously been given in any report. This is a 1045 steel, quenched into water from 1450° and drawn at 900° for one half hour. The bar from which these specimens were cut was later discarded on discovery of a flaw in the bar; however the specimens listed here do not seem to have been affected by the flaw and should be significant. The series A', A_1, A_2,

A_3, and A_4 are the same as in the first report. For convenience of reference the heat treatments are repeated here. They are all 1045 steels.

A', quenched into water from 1450° and drawn at 900° for one half hour.

A_1, "as received".

A_2, quenched into water from 1575° and drawn to 800°, (same treatment as A7 series above).

A_3, quenched into salt at 800° from 1575° (same treatment as A6 above).

A_4, quenched into salt at 1100° from 1575° (same treatment as A5 above).

These five series were all from the same original bar, different from that of A5 to A8 above.

At the end of Table VII are certain data for "Ketos" steel, obtained some time ago in my own work and not as a part of the formal Arsenal program. The interest in these data is that the steel is much harder than any of the others examined here. Ketos is a well known brand of tool steel; a typical composition as given by the manufacturers is: C 0.90, Mn 1.20, Si 0.25, Cr 0.50, W 0.50. Samples I to IV were quenched in oil and drawn at 650° F to a Rockwell C hardness of 52.5. The sample designated "glass hard" was quenched in oil and the strains relieved in boiling water, giving a Rockwell C of 65. Considerable difficulty was experienced, particularly with the glass hard steel, because of fracture elsewhere than at the narrowest part of the section because of the effect of stress concentration. The final specimen of the glass hard temper was made in the shape of a long double cone of approximately 15° double cone angle, with a straight part between the two cones, and an area at the base of the cone five times that at the narrowest section. All potential angles were rounded off. The direct measurements of a/R tabulated for specimens III and IV were made on the fractured pieces, contrary to usual practice. In these cases the shape of the fragmented pieces was such as to indicate that the error from distortion in the moment of fracture was small. The values given for a/R are each the mean of four independent measurements in four different orientations of the specimen. For one specimen the divergence from the mean of the most divergent individual reading was 12 per cent, and for the other 6 per cent. The glass hard specimen broke with no perceptible necking, although with a measureable reduction of area, and therefore with an observed a/R equal to zero.

In Table VIII revised and amplified values are given for the 9 specimens prestrained under pressure in tension and afterwards ruptured in tension at atmospheric pressure which were described in Part I of the third report. The a/R data for the first pulling under pressure of this series have already been given in Table VII. In Table VIII is given the a/R prevailing at the instant of fracture on the second pulling. Satisfactory values for this could not usually be obtained by direct observation, since there is too much distortion of the contour at the instant of fracture. The values listed were obtained as follows. It happened that the fracture of specimen A_2X was of such a character that an unusually large part of the contour was left on one of the fractured halves, so that it seemed safe to assume that the contour of this particular specimen had not been seriously distorted in the act of fracture. The a/R of this specimen was 0.72. The initial value of a/R when pulling starts at atmospheric pressure is the value given by the machining operation and was directly measured; its average value for all nine specimens was 0.15. The corrections for flow corresponding to an a/R of 0.72 and 0.15 were evaluated, and a straight line drawn through the two points in a plot of correction versus the natural strains, which were 0.93 corresponding to $\frac{a}{R}$ = 0.15, and 0.84 corresponding for a/R = 0.72. The flow correction at fracture for any particular specimen was then assumed to be the value given by the straight line, the corresponding natural strain being known. The total range for the correction factor was from 0.93 to 0.84; this range is so small that linear interpolation should not give a result anywhere in serious error. The a/R of column 5 of Table VIII is the a/R corresponding according to Table II with the linearly interpolated correction factor. The "extrapolated corrected flow stress at fracture" of column 7 is the corrected flow stress extrapolated linearly to the observed natural strain at fracture, assuming in the extrapolation the average slope of the stress-strain curve given by the series of readings below fracture. In the third report the actually observed fracture stresses were given; these are unsatisfactory, as mentioned in the report, because of difficulties of observation. The new procedure seems definitely preferable. The result is that the entries of column 7 of Table VII are always less than the "corrected true stress" at fracture given as the last entries, in parentheses, in column 7 of Table II of the third report. The other entries of Table VIII were obtained by procedures already described.

The tabulated data are now shown graphically. First the experimental values of the flow stress are shown as a function of natural strain for the series A5, A6, A7, A8, and A_2 in Figures 6 to 10. The values corresponding to non-fracture of the specimen are shown as simple circles, and the points corresponding to fractured specimens as dashed circles. The former are less subject to experimental error, and have been given somewhat greater weight in drawing the straight lines representing the stress-strain relation. It is to be commented, however, in this connection, that because of the experimental setup the points corresponding to fracture shown in Figures 6 to 10 are much less subject to error than the points determined at atmospheric pressure for the A_2 series fractured after prestraining and discussed in

Part I of the third report. The fracture points of Figure 6 to 10 were obtained in the high pressure apparatus; the tensile load itself was not measured at the instant of fracture but only the strain, and the tensile load for fracture was obtained by an extrapolation according to strain. The pre-strained specimens broken at atmospheric pressure were handled in another apparatus and the fracture stress determined from the best reading that could be made of the instantaneous tensile load at the moment of fracture. Since the load was varying rapidly just before fracture, this procedure may give considerable error, and furthermore appears to have the disadvantage of giving results consistently too high. It is for this reason that the fracture stresses of the pre-strain specimens have been revised as described on page 20.

The straight lines of Figures 6 to 10 are collected in Figure 11. Except for A6, which is slightly out of line, the usual correlation is shown between slope and absolute height of these lines. The absolute values may be expected to be somewhat different from previous values because of the effect of the correction for stress distribution across the neck. The approximate location of the line for drawn Ketos is also shown; there is, however, more uncertainty with regard to this than the others.

In Figure 12 the hydrostatic pressure prevailing at the instant of fracture is shown plotted against the natural strain at fracture. The data for five series of 1045 steel are extensive enough to justify plotting in this way. In addition, the points for drawn Ketos are also included to show what sort of effects may be expected in much harder steels. In order to be significant, the data for these curves should be obtained under comparable conditions. This demand is satisfied because the points shown all refer to specimens of the same initial proportions, broken by an uninterrupted uniform increase of tension and pressure. Obviously points obtained by any drastically different procedure, such as interrupting the application of the load and refiguring the specimen before fracture, would not be expected to lie on the curves. Thus the point for A5-A7 in Table III would not be expected to lie on the curve, as indeed it does not. It has already been found that up to the pressures at which the tensile part of the break disappears, that is, up to pressures between 200,000 and 250,000 psi in the case of the 1045 steels, the relation between natural strain at fracture and hydrostatic pressure is approximately linear. Figure 12 indicates that the relation continues approximately linear up to twice that pressure. It is true that if the points for the A5 and A6 series were considered on their own merits in isolation from the others it might be concluded not only that there is a break in the direction of the line between

200,000 and 250,000, but that there is also a break in the line itself. It is obvious from the physics of the situation, however, that the line itself must be continuous, so that the apparent discontinuity must be a chance result of the scattering of the points due to experimental error. However, the question might well receive further experimental investigation; the measurements are difficult, particularly at high pressure where necking is great and the distortion in the act of fracture great enough to introduce error into the determination even of the correct neck diameter and hence of the natural strain at the instant of fracture. This source of error might perhaps be smothered by making many experiments. It is also to be remarked that similar sets of measurements are in process of being made on a number of different steels for the N.D.R.C. and one of these shows a disturbance of slope at high pressures which possibly is not accidental. For the present the only justifiable conclusion would seem to be that there is at any rate no large disturbance of the slope of the curve plotting natural strain at fracture against pressure at which fracture occurs on passing through the pressure where the tensile part of the fracture disappears. This conclusion holds whether or not the curve is linear. The points both for the A8 series and for drawn Ketos lie smoothly on curves concave toward the axis of strain; the number of examples is too small to judge whether this departure from linearity may be due to accidental error or not.

In Figure 13 the ratio of the area of the tensile fracture to the total area of the neck is plotted against the hydrostatic pressure at the instant of fracture. The matter has already been discussed in an N.D.R.C. report; these new results agree qualitatively with those previously found. The tensile part of the fracture disappears at high pressures; at lower pressures there is an approximately linear relation between the pressure at which fracture occurs and the ratio of the areas. If there is any consistent deviation from linearity it is probably in the direction of convexity toward the pressure axis, which would mean some indefiniteness in the pressure at which the tensile fracture vanishes. This is suggested most strongly by the A5 series above; however the scattering of the points is too great to make this conclusion secure. Figure 13 suggests that there may be a correlation between the pressure at which tensile fracture disappears and the strain-hardening curves of Figure 11, the pressure of disappearance being greater the greater the slope of the strain-hardening curve and the greater the absolute value of the flow stress. A correlation of this sort is made much more probable on including the results for the drawn Ketos. One might perhaps also expect a correlation with the appearance of the fracture at atmospheric pressure, but in this regard the results are not unambiguous. In the 1045 steels the tensile part of the fracture at atmospheric pressure becomes less extensive in the direction of increasing hardness (the A7 series has the smallest ratio at atmospheric pressure), but the direction of variation of the ratio reverses and increases to nearly unity on passing to the Ketos steel.

An attempt was made to answer the question whether the disappearance of the tensile fracture above a certain pressure is a legitimate pressure effect, or whether it is associated with the change of shape (increasing a/R) which accompanies increase of pressure, by artifically changing the geometrical shape. Specimen A5-A7 (Table III) was first pulled to a strain of 1.69 under a hydrostatic pressure of 227,000 psi. This is safely below the fracture point, which at this pressure may be expected to occur at a strain of 3.2 (Figure 12). Pressure was now released and the specimen machined to the shape of a double cone as indicated in Figure 14. The angle between the generating lines of the cone and the axis was 8.8°. The generating lines of the opposed cones were not continued to intersection but the intersection was rounded to a circular contour with a/R equal to 0.078. In the machining the diameter at the narrowest part was reduced from 0.175 to 0.169 cm. The surface was polished and made as free from scratches as possible.

The angle of the cone was not made smaller for fear that the fracture would not come at the original neck; it is known that if a specimen which has been necked in tension is refigured by giving it a cylindrical figure the fracture on the second pulling will not occur at the original neck, an obvious result of inhomogeneous strain-hardening. After machining the specimen was replaced in the pressure apparatus and broken in tension at a pressure of 267,000 psi, somewhat higher than the previous pressure and not far from the pressure at which Figure 13 would indicate that the tensile break should entirely disappear. The additional strain to fracture on the second pulling was 2.74, making a total strain at fracture of 4.43, and the a/R at fracture was of the order of 1.0, a figure which could be established only roughly by examination of the fragmented segments. This value of a/R, crude as it doubtless is, is nevertheless impossibly out of line with the value that would be associated with a strain of either 2.74 or 4.43 attained with a single application of pressure (see Figure 5), thus showing the effectiveness of the refiguring operation in drastically changing the geometry. The point now is that the fracture was entirely shearing in character; if the specimen had been broken on the initial application of pressure at a strain of 2.74 a hydrostatic pressure of about 175,000 psi would have been necessary (Figure 12), and at this pressure about 0.1 of the neck area or 0.3 of the neck diameter would have been occupied by the tensile fracture. Or if the fracture on the initial application had occurred when a/R had attained a value of 1, about 0.4 of the neck area would have been occupied by the tensile fracture. According to either method of computation it would thus appear that the disappearance of the tensile break and the assumption of exclusively shearing characteristics is at least in large part a legitimate pressure effect, and is not associated exclusively with the incidental geometry. Another method of attack was applied to the same question. A virgin specimen of the A6 series was machined so as to have the shape of a specimen necked by pulling under hydrostatic pressure to an a/R value of 1.86. It will be found from the data given for the A6 series that when pulled under pressure the tensile fracture disappears for values of a/R greater than 1.75. The virgin specimen with the artificial neck was now broken at atmospheric pressure. The fracture was of the conventional cup-cone type and the tensile part of the fracture occupied 43 per cent of the cross section, which according to Figure 13 is approximately the value for a conventional straight tensile specimen fractured at atmospheric pressure. This result in itself would be nearly conclusive. In conjunction with the same conclusion reached by the other method of attack we may accept as established that the change in the character of the fracture is primarily a legitimate pressure effect.

The progressive change in the character of the fracture with increasing pressure is shown by the photographs in Figures 15 to 20 for the A6 series. There is a progressive change in several features of the fracture. The area of the tensile part of the cup-cone (flat bottom of the cup) becomes less with increasing pressure, vanishing altogether in Figure 19 and 20. A feature not brought out by these photographs, but well shown in a series of longitudinal sections made for the N.D.R.C., is that the tensile part of the break is always accurately situated at the narrowest part of the neck. The fracture becomes finer grained with increasing pressure, both on the tensile and the shearing parts; the shearing part eventually becomes brightly burnished. Up to the disappearance of the tensile break the shearing part of the fracture is situated on a cone, segments of which may be divided between the two halves of the specimen. At pressures above the disappearance of the tensile break, however, the shearing fracture rearranges itself and ultimately takes place on a single plane, which is highly burnished. The angle of the shear with the axis is not constant in the range where the shear is situated on cones, but a longitudinal section shows curved surfaces of shearing slip, which under some conditions may give contours like the vortex of a whirlpool, running down into tubular extensions approaching parallelism with the axis. This is suggested in Figure 21, which indicates what happens when the cup part of the fracture is divided between the two halves, or when it is all attached to one half. The two halves do not fit together. Apparently the edge of the cup gets dragged out by the tensile force after it has parted company at the center with the other half, while the parts still in contact are sliding over each other, pressed together by the hydrostatic pressure and thus being burnished. Under high pressure cohesion across surfaces slipping over each other in shear may be practically unimpaired, as shown by some experiments on punching under pressure not yet published. A hypothetical intermediate stage of the fracture, before separation of the halves is complete, is suggested in Figure 22. During the process of separation the external pressure is tending to collapse the cavity from the sides; this effect will become increasingly important at high pressures. The combination of collapse by pressure and dragging out by tensile force indicates the possibility of considerable distortion in the act of fracture, and of considerable difference in shape of the two halves.

The principal stress components at fracture are given in columns 9, 10, and 11 of Tables III to VIII, and in column 12 is one third the sum of the principal components, or the mean hydrostatic tension. In

Figures 6 to 10 there are plotted, in addition to the flow stresses, $\widehat{zz}$, the longitudinal tensile component of stress or column 11, which is at the same time the maximum tensile component, and also the mean hydrostatic tension or column 12. The irregularities in $\widehat{zz}$ are somewhat greater than the irregularities in the flow stress; this is not surprising because $\widehat{zz}$ is somewhat more remote from the results of direct measurement, since the corrections for stress distribution arising from necking are greater for $\widehat{zz}$ than for flow stress. In spite of the irregularities, however, the general trend of $\widehat{zz}$ is quite unmistakable; it rises with increasing strain roughly parallel to the flow stress, and appears in general to be somewhat larger than the flow stress. The increase of $\widehat{zz}$ in the range of measured strains is large; for example the increase for the A5 series is by a factor of the order of magnitude of 4. This would seem to make conclusive the absolute untenability of the old maximum tensile stress criterion of fracture. Incidentally the untenability of the maximum shearing stress criterion of fracture is also demonstrated by inspection of the figures. It seemed hardly worth while to make a special tabulation of the maximum shearing stress, which is $\widehat{zz} - \widehat{rr}$, but inspection will readily show examples of variations of several fold.

The diagrams show that the mean hydrostatic tension, that is, one third the sum of the principal stresses, is approximately constant at fracture. A study of the distribution of irregularities gives even greater weight to this statement than a cursory examination of the points themselves, because it will be seen that departures from constancy of the mean tension are often correlated with deviations in the same direction of the flow stress, and are thus probably associated with errors of observation or with flaws in the particular specimen. Examples of this correlation are the two points of the A5 series at strains of 1.13 and 1.56, and two points of the A6 series at strains of 2.37 and 2.78. The probablility that there is something fundamental in the constancy of the mean tension is made much more impressive by the behavior of several exceptional specimens. Specimen A5-A7 was, as already described, broken on the second pulling after refiguring, so that it broke at a value of a/R and a value of mean tension on the axis arising from necking quite out of the ordinary run. Nevertheless its mean tension at fracture differs from that of other specimens fractured under routine conditions by no more than the experimental irregularity (point at strain of 4.43 in Figure 6). Even more striking is the behavior of the specimens broken at atmospheric pressure after preliminary straining under pressure, given in Table VIII. The points for all the fractured specimens of the A_2 series are plotted together in

Figure 23; the mean hydrostatic tension is the same within the limits of error both for the prestrained specimens and for those broken on the initial application of pressure.

It is to be remarked that modification will be required in some of the statements of the third report to the Arsenal on the fracture of prestrained specimens; that report was written before the role of all the components of stress in determining fracture was appreciated.

Assuming now that the criterion of fracture is that the mean hydrostatic tension shall reach a critical value, we speculate on some of the consequences. In the first place, what happens when the mean tension reaches a critical value is that the volume has been distended to a definite amount; this is in virtue of the approximate constancy of the bulk modulus. It is true that the constancy of the bulk modulus in the plastic range appears never to have been established by direct experiment, but it is usually assumed to be true and it appears plausible enough. This means, then, that when the volume has been distended by a critical amount the structure becomes unstable. It is to be asked whether this critical distension may not possibly be sensitive to temperature, so that increasing values of the mean tension at low temperatures may be looked for. As a rough mean value for the critical mean tension we may take 125,000 psi from the measurements above. This gives a volume distension of 0.005, numerically equal to the volume contraction on cooling through 140°C.

The process by which the conditions of fracture are reached would seem to be somewhat as follows. If the specimen is pulled at atmospheric pressure necking starts when the extension has reached such a value that the slope of the strain-hardening curve has dropped below a critical value. As stretching proceeds the flow stress builds up and simultaneously the curvature of the contour and with it the radially symmetric stress on the axis increases. This process continues until the mean of the principal stresses on the axis, called the mean hydrostatic tension, reaches a critical value. If the specimen is pulled in a medium under pressure all the stress components are decreased by the pressure in the liquid, so that the strain has to proceed further until a greater flow stress arising from the increased strain-hardening at the greater strain and an increased hydrostatic tension arising from the greater necking and accompanying greater curvature together compensate for the hydrostatic pressure. If the normal process is interferred with, as by refiguring the specimen so that curvature of the contour is less than would normally be associated with the strain, then the hydrostatic tension arising from necking is less than normal and the necking process and with it the extension has to proceed further than normal to yield a mean tension equal to the critical value. In other words, it takes a greater extension to break a specimen under a given hydrostatic pressure in the ambient liquid after the specimen has been refigured to reduce the curvature of the contour. This is illustrated by the specimen A5-A7.

It is not possible to have simultaneously a linear strain-hardening curve, a linear relation between strain at fracture and the hydrostatic pressure at fracture, a constant sum of the three principal stresses at fracture, and an arbitrary connection between the curvature of the contour of the neck and strain, but there must be a relation between these. We will assume the linear relations and find what sort of a relation is demanded thereby between a/R and strain. If the relation so found checks approximately with the experimentally found relation shown in Figure 4, we may assume that there is nothing qualitatively wrong in assuming linear relations for the purposes of simplified discussions.

If the strain-hardening curve is linear,

$$\sigma = a_0 + a_1 \log A_0/A$$

The hydrostatic tension on the axis arising from necking is $F \log (1 + \frac{1}{2}\frac{a}{R})$. A linear relation between strain and hydrostatic pressure at fracture gives:

$$P = b_o + b_1 \log A_o/A$$

where a_o, a_1, b_o and b_1 are constants. The stress components on the axis at fracture are:

$$\widehat{rr} = F \log (1 + \frac{1}{2}\frac{a}{R}) - P$$

$$\widehat{\theta\theta} = F \log (1 + \frac{1}{2}\frac{a}{R}) - P$$

$$\widehat{zz} = F \left\{ 1 + \log (1 + \frac{1}{2}\frac{a}{R}) \right\} - P$$

Whence the mean hydrostatic tension, or one third the sum of the principal stress components, is:

$$\text{Mean Tension} = \frac{1}{3}\Sigma = F \left\{ \frac{1}{3} + \log (1 + \frac{1}{2}\frac{a}{R}) \right\} - P = \text{const.}$$

Since F/3 and P are both linear in the strain it follows that $F \log (1 + \frac{1}{2}\frac{a}{R})$ is also linear. We set $F \log (1 + \frac{1}{2}\frac{a}{R}) = c_o + c_1 \log A_o/A$, where c_o and c_1 are constants to be determined. a/R vanishes at the beginning of necking. Designate the strain at the beginning of necking by S_o. We have then $c_o = -c_1 S_o$, and on substituting in $\frac{1}{3}\Sigma$, c_1 is seen by inspection to be $b_1 - \frac{a_1}{3}$, giving finally:

$$\log (1 + \frac{1}{2}\frac{a}{R}) = \frac{(b_1 - a_1/3)\left\{ \log A_o/A - S_o \right\}}{a_o + a_1 \log A_o/A},$$

$$\text{Mean Tension} = \frac{1}{3}\Sigma = a_o/3 - b_o - S_o\,(b_1 - \frac{a_1}{3})$$

According to this, a/R approaches a limiting value for large strains such that $\log (1 + \frac{1}{2}\frac{a}{R}) = \frac{b_1}{a_1} - \frac{1}{3}$.

This seems not unreasonable, and consistent with Figure 4. To get a more precise check we may substitute the numerical values taken from Figures 11 and 12 for the A5 series:

$$a_o = 115,000$$
$$b_o = -95,000$$
$$a_1 = 66,000$$
$$b_1 = 100,000$$

From Figure 2 we take the value of S_o for the A5 series to be 0.3.

This gives

$$\log \left(1 + \frac{1}{2}\frac{a}{R}\right) = \frac{1.182 \left\{ \log A_o/A - 0.3 \right\}}{1.744 + \log A_o/A}$$

We make a table of values as follows:

Table IX

$\log \frac{A_o}{A}$	$\log \left(1 + \frac{1}{2}\frac{a}{R}\right)$	$\frac{a}{R}$	a/R from Figure 4
0.3	0	0	0.18
1	.302	0.70	0.77
2	.537	1.42	1.40
3	.672	1.92	1.83
4	.760	2.28	2.10
∞	1.18	4.52	

At low strains the lack of agreement is evidently due to the exceptionally high value for S_o for this series. But on the whole the agreement is not bad and indicates that there is nothing qualitatively wrong with assuming linear relationships and that approximate quantitiatve agreement may be expected over the experimental range in which the strains are not too large to vitiate the measurements by geometrical dissymetries. Particularly important is the enhanced probability indicated by this result that the constant mean tension criterion for fracture is approximately correct over a considerable range.

We made the above calculation by extrapolating the line for hydrostatic pressure at fracture backwards into the region of negative pressures. This region of course has not yet been entered experimentally, and probably a more rigorous method of finding the a/R curve implied in the linear relationships would have been to determine the constants c_0 and c_1 so as to secure agreement with the experimentally determined values for fracture at atmospheric pressure. The difference would not have been important, however, and there is a certain interest in prolonging the various lines into the negative regions. Extrapolation cannot be made with physical significance beyond the point at which necking starts, for here a/R vanishes, and for smaller strains continues to have the value zero, because in this region the specimen stretches uniformly, without necking. In other words, the straight line which represents $F \log (1 + \frac{1}{2} a/R)$

breaks at the necking point and at smaller strains coincides with the axis. Down to the strain where necking starts, there seems no reason why linear extrapolation to negative pressures should not be physically significant. The meaning of the negative pressures is merely that some other technical method must be found of exerting the spherically symmetrical part of the stress system on the specimen than by the medium of a liquid, a liquid being capable of exerting only positive pressures over any extended range. Since the line for $F \log (1 + \frac{1}{2} \frac{a}{R})$ breaks at the necking point, it is natural to suppose that the lines for P and for F also break below this point. It is of course known that the normal strain-hardening curve becomes concave downward at strains below the necking point, but this is probably not the sort of extension that is involved here. The F values which we are seeking here are such that the specimen <u>fractures</u> under the stress system $\widehat{rr} = \widehat{\theta\theta} = - P$; $\widehat{zz} = F - P$, whereas the conventional extension of the F curve relates only to a plastic extension of the specimen at constant atmospheric pressure without fracture. We may make a plausible guess as to the extension of the curves below the necking strain by considering that at a sufficiently high hydrostatic tension the specimen must fracture without strain. This point has not been demonstrated experimentally, but it is inconceivable that any material can withstand an indefinitely high tensile stress and so an indefinitely high volume distension without ultimate rupture, and it is a matter of experiment that after every known type of fracture the plastic volume strain vanishes. Since by symmetry any plastic strain at fracture under hydrostatic tension must be uniform in all directions it follows that the plastic strain of our analysis, that is log A_o/A, must vanish. If the stress for fracture is spherically symmetrical at zero strain, F at zero strain must vanish. It is simplest to assume that between zero strain and the strain at necking the F curve is a straight line running from the origin to the point at the start of necking. There seems no reason to assume that the hydrostatic tension for brittle fracture with no other stress component is not merely the constant mean tension or $\frac{1}{3}\Sigma$ that determines fracture over the entire experimental range of strain. This criterion seems to be something fundamental, and one would certainly be going out of ones way to assume that in the short range below the strain of necking this constant value is deviated from. We assume therefore that at zero strain the value of P is $-\frac{1}{3}\Sigma$ or $-\frac{a_o}{3} + b_o + S_o\,(b_1 - \frac{a_1}{3})$. We also assume as simplest that the complete P curve consists of two straight lines: above the necking point the equation is $P = b_o + b_1 \log \frac{A_o}{A}$ and between the necking point and zero strain the curve is a line joining the necking point with the point $-\frac{a_o}{3} + b_o + S_o\,(b_1 - \frac{a_1}{3})$ on the axis.

The numerical magnitude of the mean tension for rupture of the A5 series is 110,000 psi. This is considerably less than the average tensile stress at fracture at atmospheric pressure, 190,000. An examination of the figures for the other series of steels will show that this is a general result. It has usually been considered that the hydrostatic tension for fracture, often called the "cohesive strength", would be considerably higher than the conventional true tensile strength. The reversal in the order of these quantities is one of the effects of recognizing stress distribution in the neck.

Finally we make some comments on the general subject of conditions of fracture. In the first place it is obvious that an essential difference is to be anticipated between the methods of formulating any such conditions which may be applicable to a substance that breaks brittlely without plastic strain or to a ductile substance like those examined here which may permit large strains before fracture. The conditions for the fracture of a brittle material will not involve strains, but can be formulated in terms of stresses only, so that for such materials there are "fracture surfaces", that is, surfaces in the three dimensional space in which the three principal components of stress are taken as coordinates such that if the stress attains values represented by points on the surface the material fractures.

Not only may we expect that fracture surfaces for brittle materials exist, but it should be possible to actually realize any point on the surface by subjecting the material to the desired stress system by applying the proper forces to the faces of a cube, overlooking the technical difficulty of applying indefinitely high tensile forces as distinguished from pressures. The situation is much more complicated for plastic materials. Since fracture occurs with both strain and stress a complete specification of fracture demands a specification of at least both stress and strain and perhaps of other quantities. It is therefore not evident that a fracture surface like that for brittle materials even exists, that is, a surface in a three dimensional space of the principal stress components. Furthermore, a complete experimental mapping out of the conditions under which fracture may occur may conceivably encounter difficulties in principle. An arbitrary stress system cannot be realized merely by applying the indicated forces to the faces of a cubical element, not only for the reason that the material flows, but also because the material may flow unstably. A single component of stress cannot be applied arbitrarily to a tension specimen, for example, but necking starts above a certain stress and other components of stress automatically make their appearance, so that the stress field inside a material subjected to a homogeneous external force field becomes non-homogeneous and difficult of control. It would appear then that arbitrary force fields can be produced, if at all, only by special devices, such as refiguring the specimen as flow progresses, and even then it is not evident whether there are essential limitations on such indirect methods or whether anything more can be attained than the realization of an arbitrary stress at a single point. If so, the question of fracture in plastic materials is further complicated by uncertainty with regard to the role of stress gradient in determining fracture.

In view of such possible complications a most welcome simplification appears in the mean tension criterion for fracture suggested above. This is a condition on the stresses; fracture occurs when the stress system reaches a critical condition, in spite of the fact that the strains at this stress are not determinate but may have different values depending on past history. Actually, this criterion has been tested by experiment only under restricted conditions. A general formulation of the condition in rectangular coordinates would be:

$$X_x + Y_y + Z_z = \text{const.}$$

The fracture surface would therefore be a plane perpendicular to the axis of spherically symmetric or hydrostatic stress. But in all our experiments the stress has been subject to the condition that two of the components are equal, so that actually we have not established the existence of a fracture surface, but only that fracture occurs when the stress is situated on three lines in the stress space perpendicular to the axis of hydrostatic stress and symmetrically spaced around it. It is a most natural hypothesis that a plane can be stretched over the three lines. Whether this is justified should be one of the next things to examine experimentally.

If the complete fracture surface of ductile materials is the plane $X_x + Y_y + Z_z = \text{const.}$, fracture can never be produced by simple compressive forces, but one would expect indefinite plastic flow, without fracture. Experiments are under way now indicating that this may be true. Apparently this criterion would also demand that fracture never occur under simple shearing stress, but again that we should have only indefinite plastic flow. But on the other hand we have the practical possibility of punching holes in sheets of plastic material. It may well be that the actual fracture in such cases of punching is associated with inhomogeneities in the distribution of stress and strain resulting in intense local tensile stresses. The sides of a punching always exhibit tearing roughnesses. There is however definite experimental evidence* that materials exist capable of exhibiting both plastic flow and fracture under overall pressures so high (750,000 psi) that it is difficult to conceive that

*P. W. Bridgman: Proc. Amer. Acad. Arts and Sci., 71, 387, (1937).

there can be a mean tension at any single point to initiate the fracture. The criterion of constant mean tension cannot be perfectly general therefore, even for plastic materials. The criterion does appear however to be applicable over a wide range of stress conditions to steels, and the practical importance of such materials is sufficient to justify further experimental examination to find what the limitations of the criterion may be. Finally, it is to be emphasized that the criterion is for the initiation of fracture; the method of propagation of the fracture and its external appearance may vary greatly, as we have seen in our examples.

TABLE I

Results for Three Special Alloy Steels.

Designation of Steel	Maximum Hydrostatic Pressure of Pulling lb/in²	Natural Strain $\log_e A_o/A$	Flow Stress lb/in²	$\frac{a}{R}$
1315	359,000	0.22	159,000	0.20
	360,000	0.88	190,000	0.70
	267,000	1.73	242,000	1.37
	370,000	2.39	274,000	1.69
2320	325,000	0.27	188,000	0.19
	345,000	0.95	233,000	0.81
	340,000	1.71	283,000	1.31
	352,000	2.54	337,000	1.62
4140	340,000	0.33	223,000	0.17
	370,000	0.82	261,000	0.70
	365,000	1.51	303,000	1.20
	360,000	2.05	348,000	1.51

TABLE II

1 Natural Strain $\log_e \frac{A_o}{A}$	2 $\frac{a}{R}$	3 Ratio of flow Stress to average longitudinal stress	4 Ratio of hydrostatic tension on axis to average longitudinal stress
0.5	0.36	.918	.153
1.0	0.79	.852	.283
1.5	1.14	.806	.363
2.0	1.42	.775	.416
2.5	1.65	.753	.452
3.0	1.83	.737	.478
3.5	1.98	.724	.498
4.0	2.10	.714	.512

TABLE III

Summary of Tensile Measurements on A5 Series

1	2	3	4	5	6	7
Designation of Specimen	Max. Hyd. Pressure of Pulling lb/in^2	Fracture or not	Natural Strain $\log_e A_o/A$	a/R when directly measured	Flow Stress at Max. or Fracture uncorrected lb/in^2	corrected lb/in^2
A5-A1	199,000	n.f.	1.42	0.85	250,000	212,000
A5-A2	350,000	n.f.	0.43	0.21	144,000	136,000
A5-A3	18,000	f.	1.13		149,000	125,000
A5-A4	263,000	f.	4.14 (?)			
A5-A5	116,000	f.	2.14		313,000	240,000
A5-A6	410,000	n.f.	3.38	1.67	435,000	337,000
A5-A7	227,000	n.f.	1.69	0.96	296,000	245,000
Ditto refigured	267,000	f.	2.74 addition 4.43 total	1.0	606,000	496,000
A5-A8	410,000	n.f.	5.05	(broken in measurement)		
A5-A9	Atmos	f.	0.90		189,000	163,000
A5-A10	74,000	f.	1.56		225,000	180,000

TABLE III (Cont'd)

1	2	3	4	5	6	7
A5-A11	182,000	f.	2.83		396,000	295,000
A5-A12	389,000	f.	4.80			
A5-B1	389,000	n.f.	2.41	1.52	310,000	235,000
A5-B2	383,000	n.f.	0.96	0.58	207,000	183,000
A5-C1	386,000	n.f.	2.04	1.29	280,000	221,000
A5-C2	315,000	n.f.	2.81	1.54	269,000	203,000
A5-C3	333,000	n.f.	1.06	0.52	226,000	202,000

TABLE III (Cont'd)

1	8	9	10	11	12	13
Designation of Specimen	Hyd. Tension on axis arising from necking at fracture lb/in^2	Stress Components at Fracture				Ratio of Area of Tensile Break To Total Neck at Fracture
		$\widehat{rr}$ lb/in^2	$\widehat{\theta\theta}$ lb/in^2	$\widehat{zz}$ lb/in^2	$\frac{1}{3}\Sigma$ lb/in^2	
A5-A3	46,000	28,000	28,000	153,000	70,000	.35
A5-A4						0
A5-A5	133,000	17,000	17,000	257,000	97,000	.14
Ditto refigured	215,000	-52,000	-52,000	444,000	113,000	0
A5-A9	50,000	50,000	50,000	213,000	104,000	.44
A5-A10	84,000	10,000	10,000	190,000	70,000	.21
A5-A11	186,000	4,000	4,000	299,000	102,000	.09
A5-A12						0

TABLE IV

Summary of Tensile Measurements on A6 Series

1	2	3	4	5	6	7
Designation of Specimen	Max. Hyd. Pressure of Pulling lb/in²	Fracture or not	Natural Strain $\log_e A_o/A$	Measured a/R	Flow Stress at Max. or fracture uncorrected lb/in²	corrected lb/in²
A6-A1	186,000	f.	2.78		340,000	253,000
A6-A2	269,000	f.	3.87			
A6-A3	145,000	f.	2.37		474,000	358,000
A6-A4	385,000	n.f.	2.25	1.77	360,000	267,000
A6-A5	34,000	f.	1.10		250,000	210,000
A6-A6	387,000	f.	4.61			
A6-A7	Atmos	f.	0.81		206,000	180,000
A6-A8	302,000	n.f.	0.51	0.21	176,000	167,000
A6-A9	366,000	n.f.	1.59	1.14	303,000	243,000
A6-C1	384,000	n.f.	3.22	1.80	457,000	338,000
A6-C2	385,000	n.f.	1.17	0.81	250,000	213,000

TABLE IV (Cont'd)

1	8	9	10	11	12	13
Designation of Specimen	Hyd. Tension on axis arising from necking at fracture lb/in^2	Stress Components at Fracture $\widehat{rr}$ lb/in^2	$\widehat{\theta\theta}$ lb/in^2	$\widehat{zz}$ lb/in^2	$\frac{1}{3}\Sigma$ lb/in^2	Ratio of Area of Tensile Break To Total Neck at Fracture
A6-A1	159,000	-27,000	-27,000	226,000	57,000	.05
A6-A2						0
A6-A3	209,000	64,000	64,000	422,000	183,000	.12
A6-A5	77,000	43,000	43,000	253,000	113,000	.40
A6-A6						0
A6-A7	50,000	50,000	50,000	230,000	110,000	.44

TABLE V

Summary of Tensile Measurements on A7 Series

1	2	3	4	5	6	7
Designation of Specimen	Max. Hyd. Pressure of Pulling lb/in^2	Fracture or not	Natural Strain $\log_e A_o/A$	Measured a/R	Flow Stress at Max. or fracture	
					uncorrected lb/in^2	corrected lb/in^2
A7-A1	Atmos	f.	0.85		337,000	294,000
A7-A2	330,000	n.f.	2.35	1.66	609,000	457,000
A7-A3	130,000	f.	1.54		416,000	335,000
A7-A4	365,000	n.f.	0.57	0.53	321,000	286,000
A7-A5	173,000	f.	2.11		570,000	440,000
A7-A6	394,000	f.	3.95			
A7-A7	60,000	f.	1.28		384,000	317,000
A7-A8	269,000	f.	2.98		796,000	588,000
A7-B1	273,000	f.	2.76		680,000	507,000

TABLE V (Cont'd)

1	8	9	10	11	12	13
Designation of Specimen	Hyd. Tension on axis arising from necking at fracture lb/in^2	Stress Components at Fracture $\widehat{rr}$ lb/in^2	$\widehat{\theta\theta}$ lb/in^2	$\widehat{zz}$ lb/in^2	$\frac{1}{3}\Sigma$ lb/in^2	Ratio of Area of Tensile Break To Total Neck at Fracture
A7-A1	84,000	84,000	84,000	378,000	182,000	0.36
A7-A3	155,000	25,000	25,000	360,000	137,000	0
A7-A5	242,000	69,000	69,000	509,000	216,000	0.03
A7-A6						0
A7-A7	128,000	68,000	68,000	385,000	174,000	0.18
A7-A8	380,000	111,000	111,000	699,000	307,000	.03
A7-B1	318,000	45,000	45,000	552,000	214,000	0

TABLE VI

Summary of Tensile Measurements on A8 Series

Designation of Specimen	Max. Hyd. Pressure of Pulling lb/in^2	Fracture or not	Natural Strain $\log_e A_o/A$	Measured a/R	Flow Stress at Max. or Fracture uncorrected lb/in^2	Flow Stress at Max. or Fracture corrected lb/in^2
A8-A2	Atmos	f.	0.98		227,000	194,000
A8-A3	382,000	n.f.	2.28	1.60	408,000	310,000
A8-A4	63,000	f.	1.39		305,000	248,000
A8-A5	348,000	n.f.	0.74	0.48	223,000	202,000
A8-A6	159,000	f.	2.10		369,000	284,000
A8-A7	407,000	f.	5.05			
A8-A9	295,000	f.	3.67			

Table VI (Cont'd)

1	8	9	11	11	12	13
Designation of Specimen	Hyd. Tension on axis arising from necking at fracture lb/in²	Stress Components at Fracture $\widehat{rr}$ lb/in²	$\widehat{\theta\theta}$ lb/in²	$\widehat{zz}$ lb/in²	$\frac{1}{3}\Sigma$ lb/in²	Ratio of Area of Tensile Break To Total Neck at Fracture
A8-A2	64,000	64,000	64,000	258,000	129,000	0.47
A8-A4	107,000	44,000	44,000	292,000	127,000	0.39
A8-A6	156,000	-3,000	-3,000	281,000	92,000	0.19
A8-A7						0
A8-A9						0

TABLE VII

Revised Tensile Data for Specimens of Previous Reports

1	2	3	4	5	6	7
Designation of Specimen	Max. Hyd. Pressure of Pulling lb/in^2	Fracture or not	Natural Strain $\log_e A_o/A$	Measured a/R	Flow Stress at Max. or Fracture uncorrected lb/in^2	Flow Stress at Max. or Fracture corrected lb/in^2
A'I	Atmos	f.	0.98		320,000	272,000
A'II	411,000	n.f.	3.17		622,000	455,000
A'III	373,000	n.f.	0.89		324,000	281,000
A'IV	408,000	n.f.	1.99		468,000	362,000
A'V	393,000	n.f.	1.38		386,000	314,000
A_1I	Atmos	f.	0.78		176,000	155,000
A_1II	398,000	n.f.	2.74	2.06	384,000	275,000
A_1III	410,000	n.f.	0.89	0.54	210,000	187,000
A_1IV	401,000	n.f.	2.01		330,000	257,000
A_1V	389,000	n.f.	1.40	0.97	265,000	220,000
A_1VI	430,000	n.f.	3.48		?	?

TABLE VII (Cont'd)

1	2	3	4	5	6	7
A_1VII	300,000	n.f.	2.10		324,000	250,000
A_1VIII	405,000	n.f.	2.30		355,000	272,000
A_2I	Atmos	f.	0.88		305,000	264,000
A_2II	395,000	n.f.	3.34		655,000	475,000
A_2III	350,000	n.f.	0.75		324,000	286,000
A_2IV	345,000	n.f.	1.63		455,000	361,000
A_2VI	Atmos	f.	0.39		296,000	58,000
A_2VII	112,000	f.	1.63		382,000	304,000
A_2VIII	208,000	f.	2.57		575,000	431,000
A_2IX	383,000	f.	3.73		773,000	557,000
A_2X	357,000	n.f.	1.09	0.92	355,000	296,000
A_2XI	357,000	n.f.	0.22	0.13	206,000	200,000
A_2XII	346,000	n.f.	2.43	1.67	518,000	388,000
A_2XIII	218,000	n.f.	1.92	1.45	445,000	343,000
A_2XIV	221,000	n.f.	1.02	0.84	335,000	282,000

TABLE VII (Cont'd)

1	2	3	4	5	6	7
A_2XV	217,000	n.f.	0.19	0.10	218,000	213,000
A_2XVI	115,000	n.f.	0.88	0.76	295,000	253,000
A_2XVII	116,000	n.f.	1.35	1.18	348,000	280,000
A_2XVIII	95,000	n.f.	0.22	0.19	210,000	200,000
A_3II	Atmos	f.	0.92		214,000	184,000
A_3III	405,000	n.f.	2.75		415,000	310,000
A_3IV	340,000	n.f.	0.79		209,000	183,000
A_3V	388,000	n.f.	1.39		288,000	235,000
A_4I	Atmos	f.	0.89		189,000	163,000
A_4II	405,000	n.f.	2.65		385,000	288,000
A_4III	350,000	n.f.	0.77		201,000	178,000
A_4IV	393,000	n.f.	1.49		270,000	217,000
AII	390,000	n.f.	3.43	1.95	(577,000	414,000)
AIII	390,000	n.f.	0.90	0.87	305,000	255,000
AIV	380,000	n.f.	1.78	1.41	417,000	325,000

TABLE VII (Cont'd)

1	2	3	4	5	6	7
Ketos I	Atmos	f.	0.07		Stresses not measured	
Ketos II	82,000	f.	0.22		351,000	340,000
Ketos III	270,000	f.	0.98	0.74	610,000	522,000
Ketos IV	334,000	f.	1.43	0.89	640,000	518,000
Ketos Glass-hard	370,000	f.	0.07	0	547,000	547,000

TABLE VII (Cont'd)

1	8	9	10	11	12	13
Designation of Specimen	Hyd. Tension on axis arising from necking at fracture lb/in^2	Stress Components at Fracture $\widehat{rr}$ lb/in^2	$\widehat{\theta\theta}$ lb/in^2	$\widehat{zz}$ lb/in^2	$\frac{1}{3}\Sigma$ lb/in^2	Ratio of Area of Tensile Break To Total Neck at Fracture
A'I	91,000	91,000	91,000	363,000	182,000	
A_1I	41,000	41,000	41,000	196,000	93,000	
A_2I	79,000	79,000	79,000	343,000	167,000	
A_2VI	77,000	77,000	77,000	335,000	163,000	0.36
A_2VII	145,000	33,000	33,000	337,000	134,000	0.12
A_2VIII	261,000	53,000	53,000	484,000	197,000	0
A_2IX	393,000	10,000	10,000	567,000	196,000	0
A_3II	58,000	58,000	58,000	242,000	119,000	
A_4I	49,000	49,000	49,000	212,000	103,000	

TABLE VII (Cont'd)

1	8	9	10	11	12	13
Ketos I						0.94
Ketos II	16,000	-65,000	-65,000	275,000	48,000	0.72
Ketos III	173,000	-99,000	-99,000	425,000	75,000	0.41 (?)
Ketos IV	230,000	-104,000	-104,000	415,000	69,000	0.43
Ketos Glass-hard	0	-370,000	-370,000	177,000	-188,000	0.75

TABLE VIII

Data for Specimens Broken after Prestraining in Tension

1	2	3	4	5	6
Designation of Specimen	$\log_e A_o/A$ on first pulling	Additional $\log_e A_o/A$ to fracture	Total $\log_e A_o/A$ at fracture	a/R at fracture	Max. flow stress on first pulling (corrected) lb/in^2
A_2X	1.09	0.84	1.93	0.72	296,000
A_2XI	0.22	0.89	1.10	0.75	200,000
A_2XII	2.43	0.51	2.94	0.50	388,000
A_2XIII	1.92	0.46	2.38	0.47	343,000
A_2XIV	1.02	0.67	1.63	0.60	281,000
A_2XV	0.19	0.76	0.96	0.67	212,000
A_2XVI	0.88	0.59	1.47	0.55	252,000
A_2XVII	1.35	0.50	1.85	0.50	279,000
A_2XVIII	0.22	0.78	1.01	0.68	200,000

TABLE VIII (Cont'd)

1	7	8	9	10	11	12
Designation of Specimen	Extrapolated corrected flow stress at fracture lb/in^2	Hyd. Tension on Axis arising from Necking at Fracture lb/in^2	Stress Components at Fracture $\widehat{rr}$ lb/in^2	$\theta\theta$ lb/in^2	$\widehat{zz}$ lb/in^2	$\frac{1}{3}\Sigma$ lb/in^2
A_2X	325,000	99,000	99,000	99,000	424,000	207,000
A_2XI	276,000	88,000	88,000	88,000	364,000	180,000
A_2XII	345,000	77,000	77,000	77,000	522,000	192,000
A_2XIII	326,000	68,000	68,000	68,000	394,000	177,000
A_2XIV	306,000	81,000	81,000	81,000	387,000	183,000
A_2XV	270,000	78,000	78,000	78,000	348,000	168,000
A_2XVI	300,000	72,000	72,000	72,000	372,000	172,000
A_2XVII	304,000	68,000	68,000	68,000	372,000	169,000
A_2XVIII	270,000	80,000	80,000	80,000	350,000	170,000

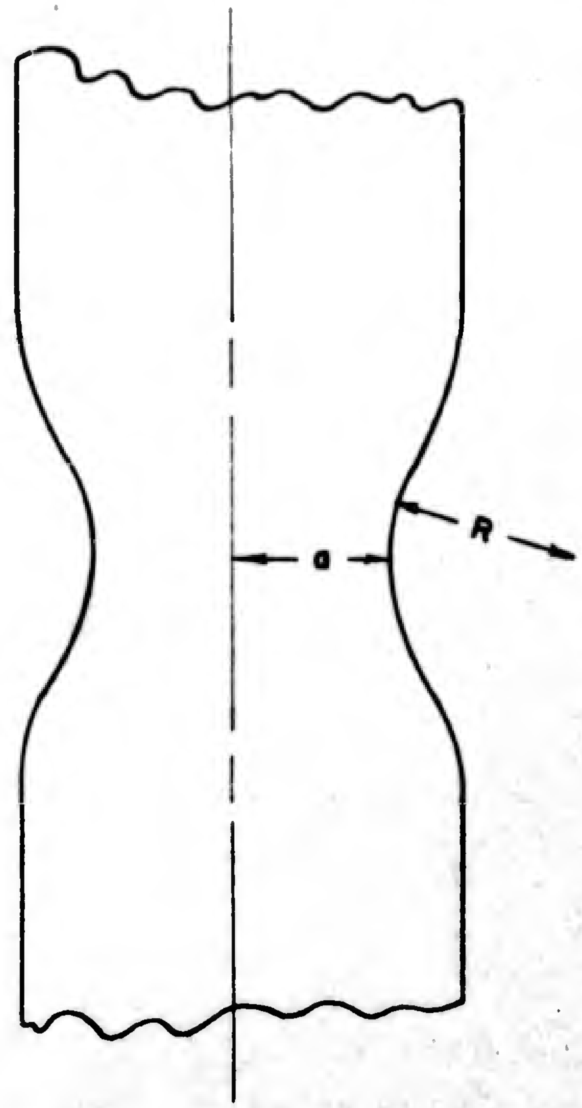

FIG. 1
THE NECK OF THE TENSION SPECIMEN

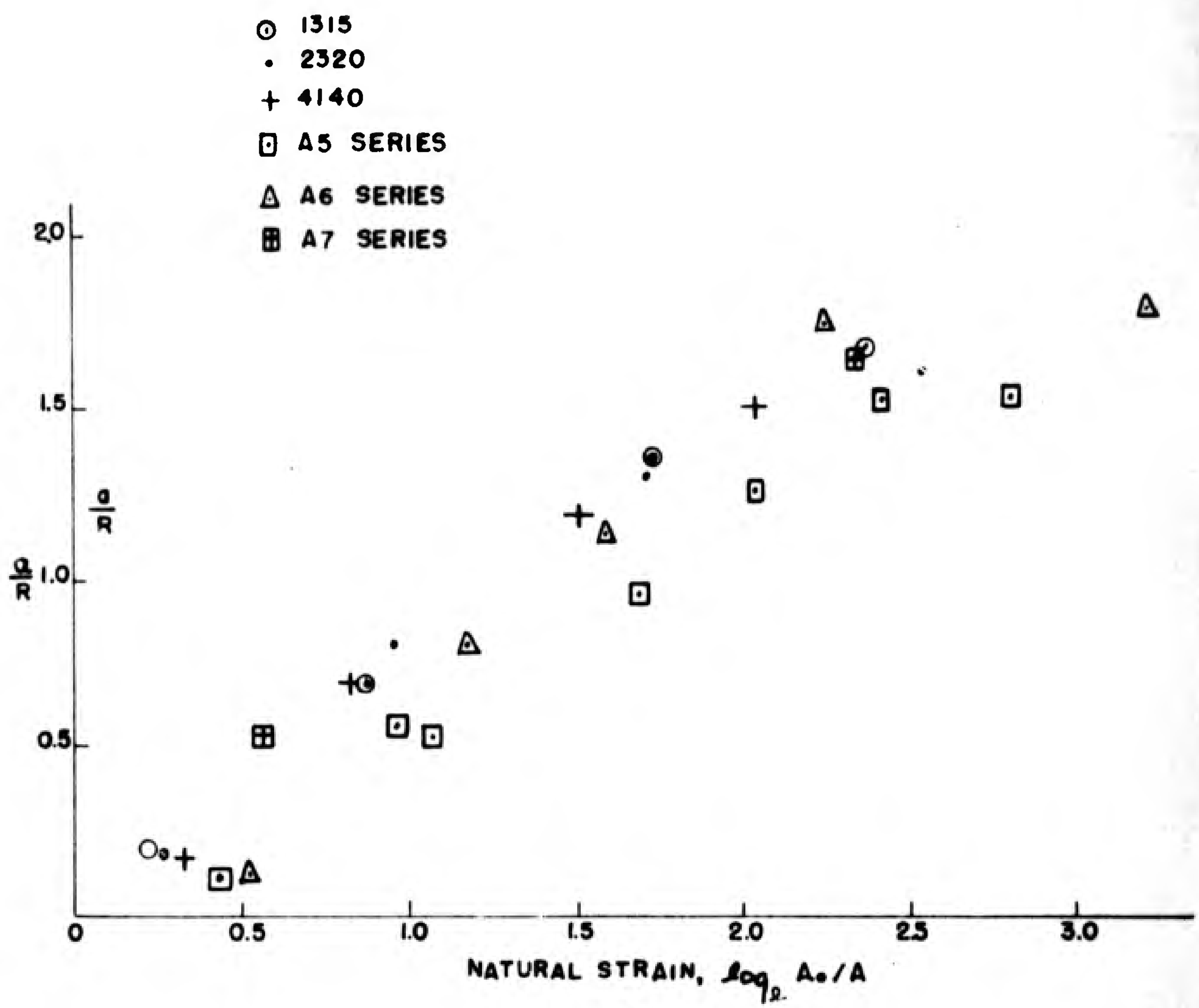

1315
2320
4140
A5 SERIES
A6 SERIES
A7 SERIES
2.0
1.5
1.0
0.5
a/R
0
0.5
1.0
1.5
2.0
2.5
3.0
NATURAL STRAIN, $\log_e A_o/A$

FIG. 2

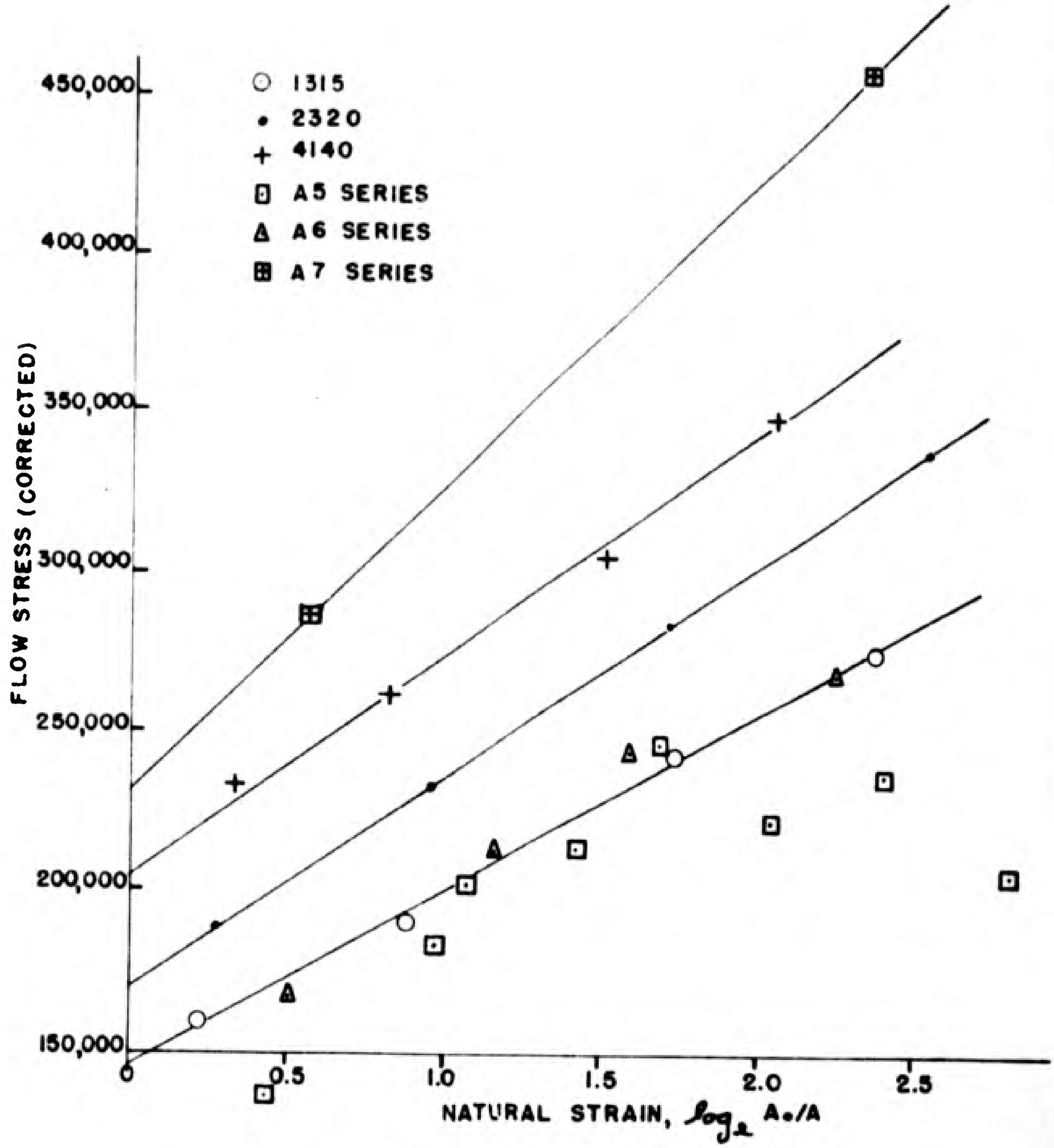

450,000
400,000
350,000
300,000
250,000
200,000
150,000
FLOW STRESS (CORRECTED)
1315
2320
4140
A5 SERIES
A6 SERIES
A7 SERIES
0
0.5
1.0
1.5
2.0
2.5
NATURAL STRAIN, loge Ao/A

FIG. 3

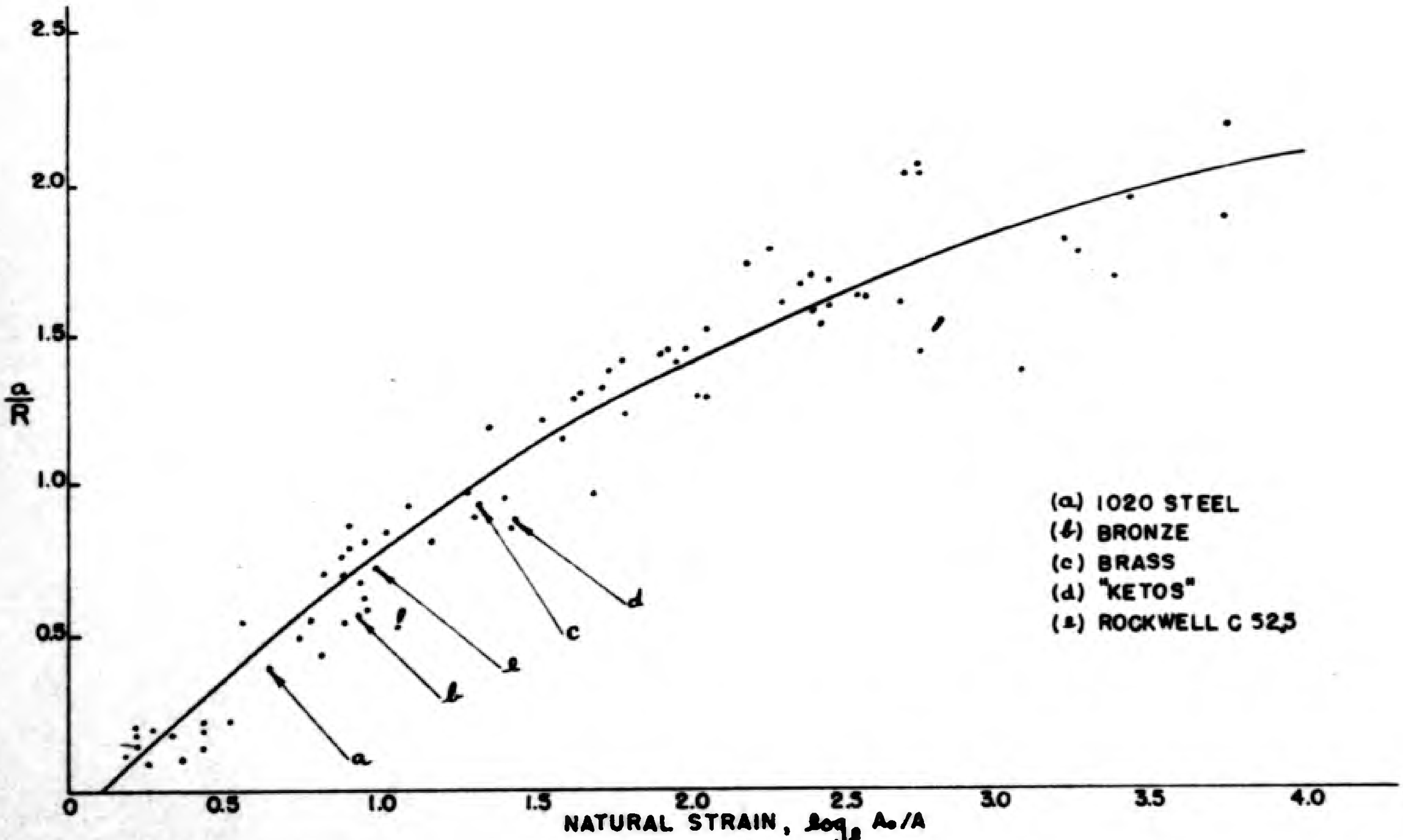

2.5
2.0
1.5
1.0
0.5
a/R
0
0.5
1.0
1.5
2.0
2.5
3.0
3.5
4.0
NATURAL STRAIN, log A₀/A
(a) 1020 STEEL
(b) BRONZE
(c) BRASS
(d) "KETOS"
(e) ROCKWELL C 52.5
a
b
c
d
e

FIG. 4

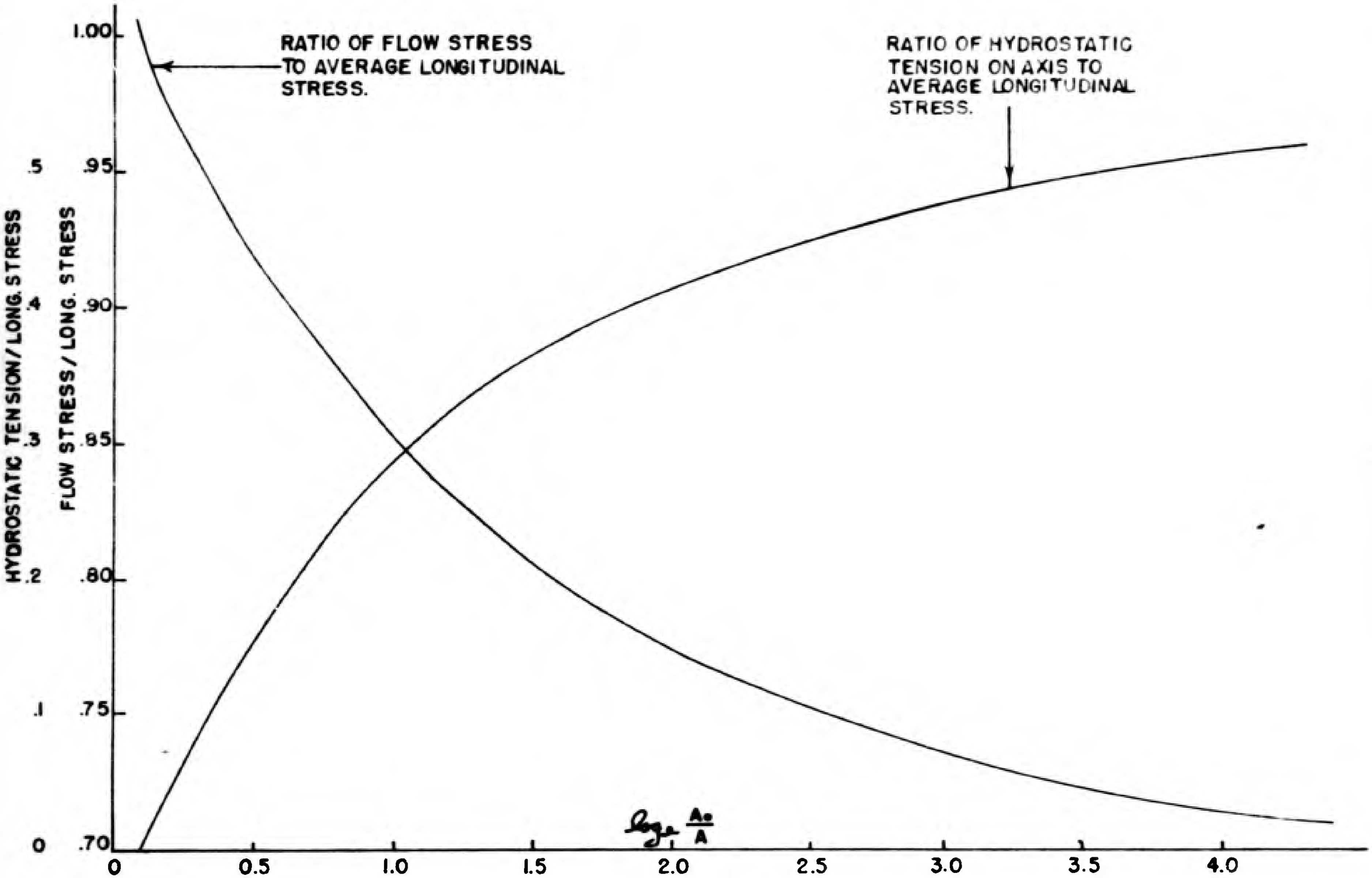

RATIO OF FLOW STRESS TO AVERAGE LONGITUDINAL STRESS.
RATIO OF HYDROSTATIC TENSION ON AXIS TO AVERAGE LONGITUDINAL STRESS.
HYDROSTATIC TENSION/LONG. STRESS
FLOW STRESS/LONG. STRESS
1.00
.95
.90
.85
.80
.75
.70
.5
.4
.3
.2
.1
0
0
0.5
1.0
1.5
2.0
2.5
3.0
3.5
4.0

FIG. 5

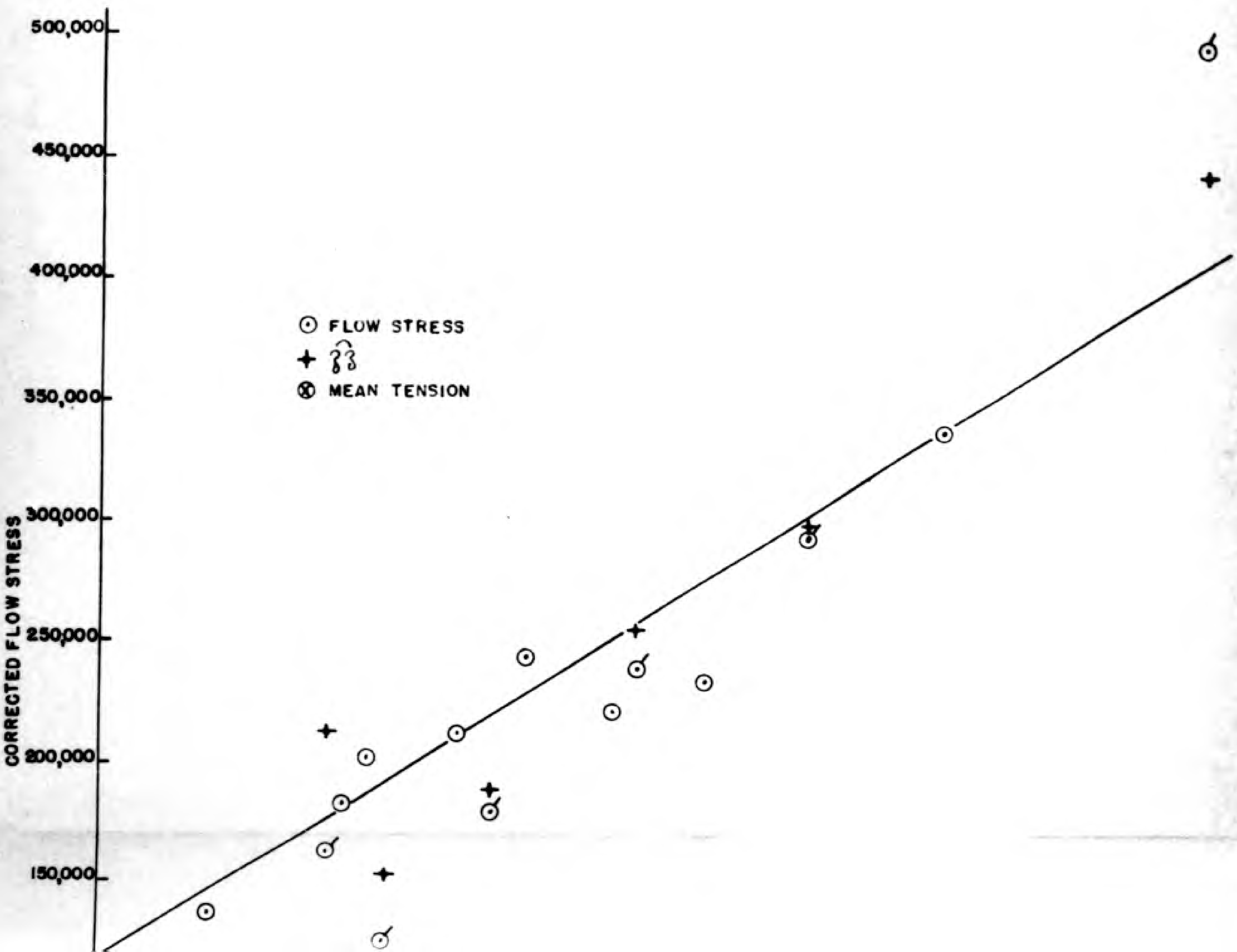

500,000
450,000
400,000
350,000
300,000
250,000
200,000
150,000
CORRECTED FLOW STRESS
FLOW STRESS
MEAN TENSION

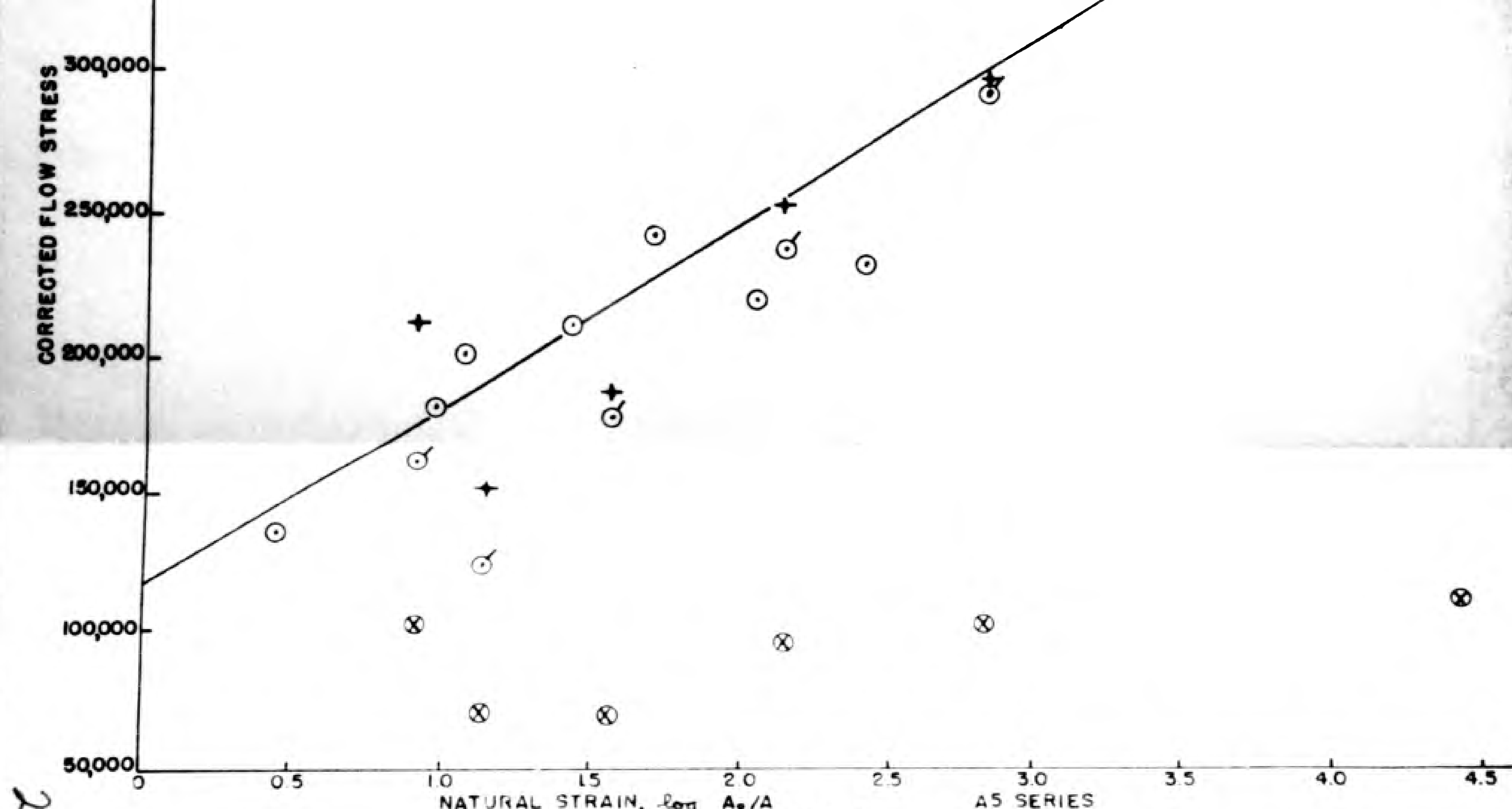
CORRECTED FLOW STRESS
300,000
250,000
200,000
150,000
100,000
50,000
0
0.5
1.0
1.5
2.0
2.5
3.0
3.5
4.0
4.5
NATURAL STRAIN, loge Ao/A
AS SERIES

FIG. 6

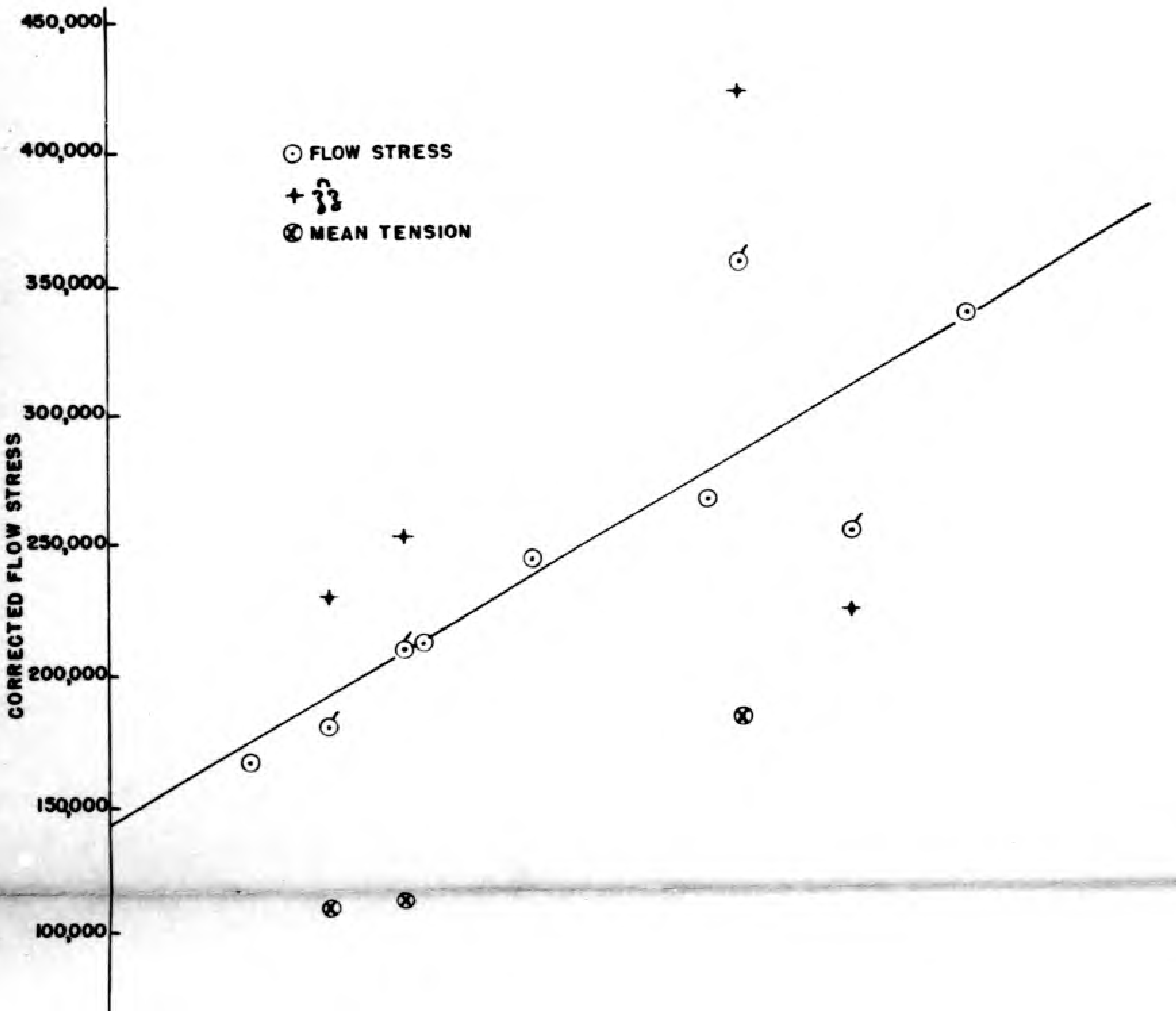

450,000
400,000
350,000
300,000
250,000
200,000
150,000
100,000
CORRECTED FLOW STRESS
FLOW STRESS
MEAN TENSION

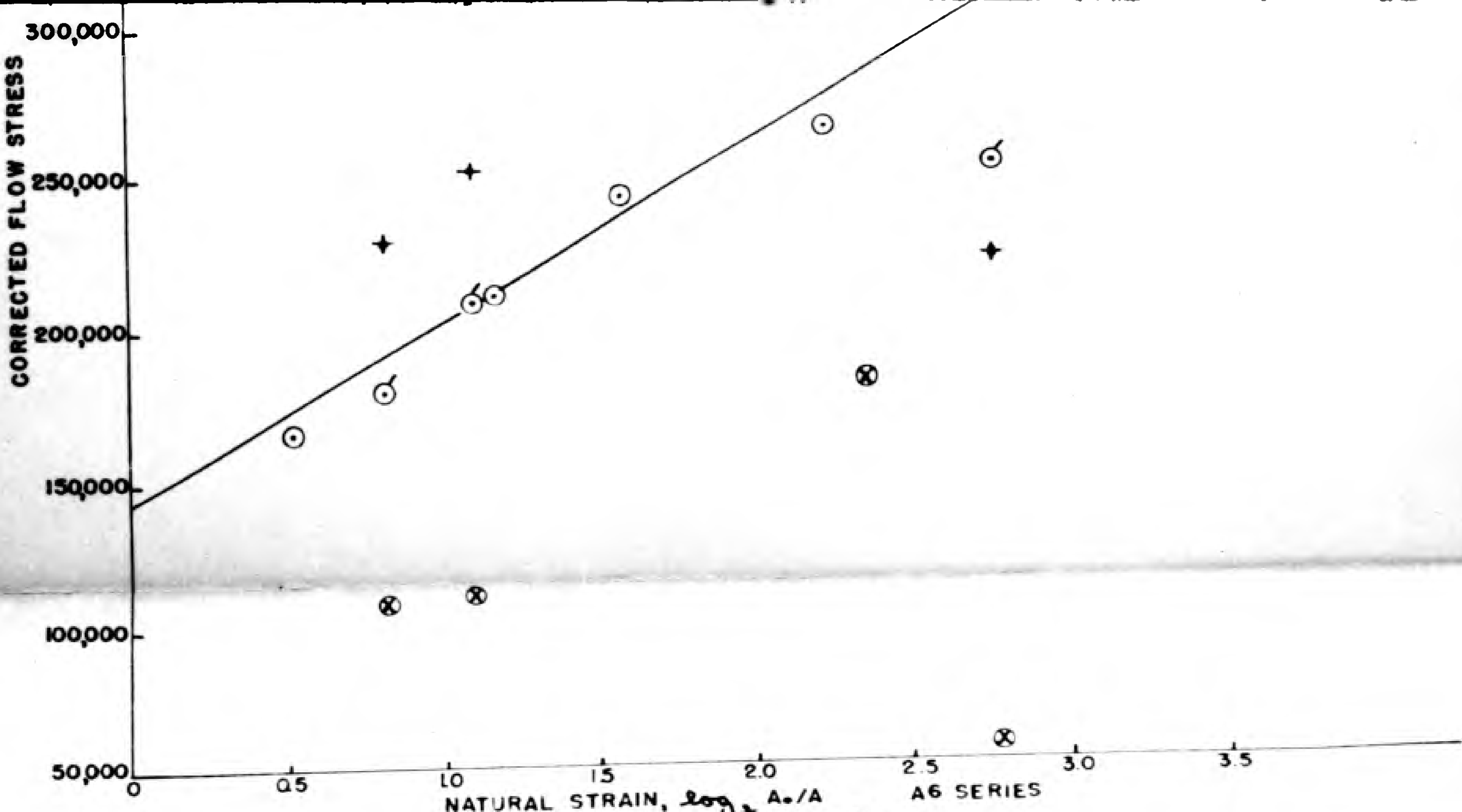
300,000
250,000
200,000
150,000
100,000
50,000
CORRECTED FLOW STRESS
0
0.5
1.0
1.5
2.0
2.5
3.0
3.5
NATURAL STRAIN, log_e A₀/A
A6 SERIES

FIG. 7

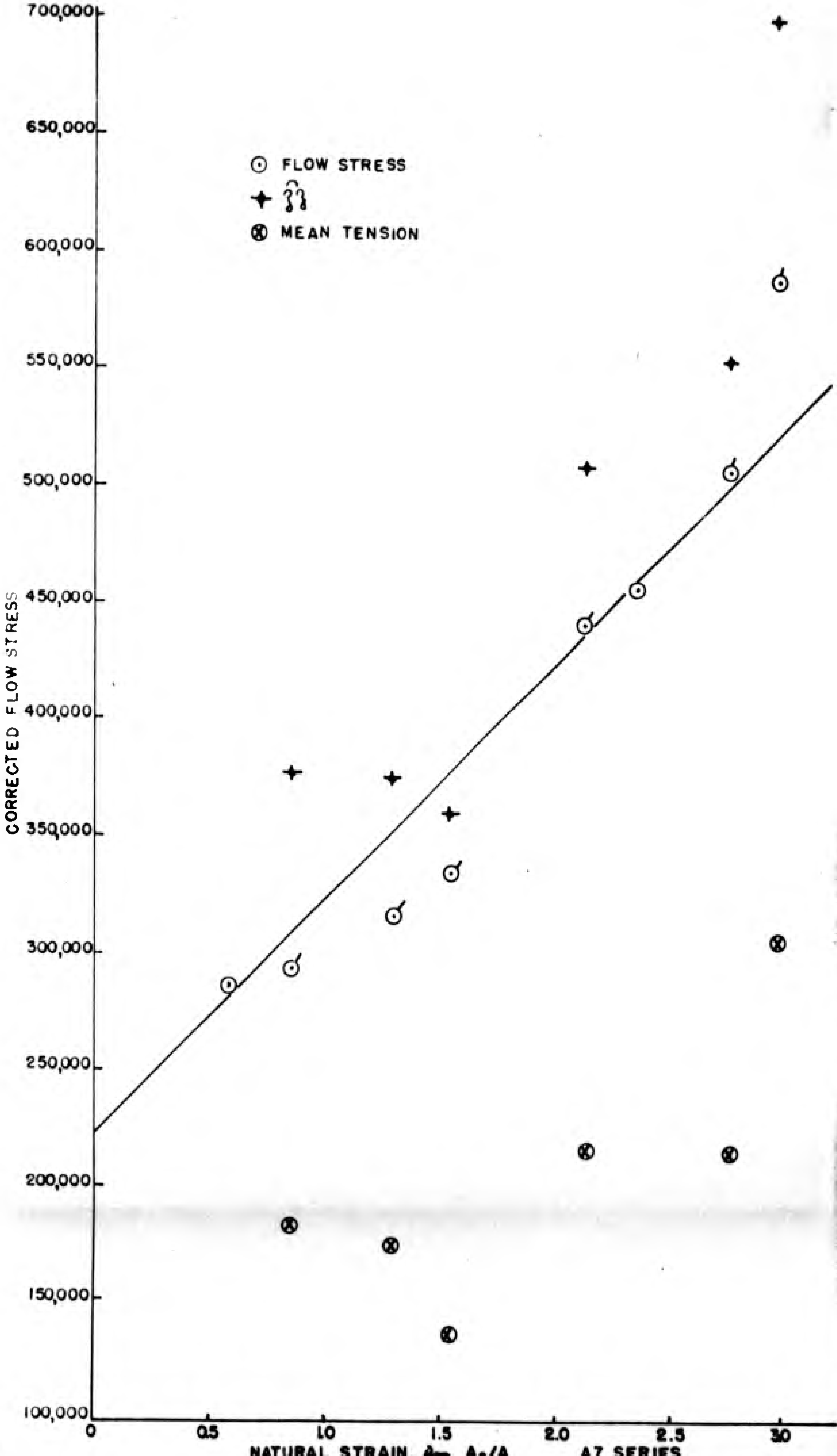
FLOW STRESS
MEAN TENSION
CORRECTED FLOW STRESS
700,000
650,000
600,000
550,000
500,000
450,000
400,000
350,000
300,000
250,000
200,000
150,000
100,000
0
0.5
1.0
1.5
2.0
2.5
3.0
NATURAL STRAIN, A./A
A7 SERIES

FIG. 8

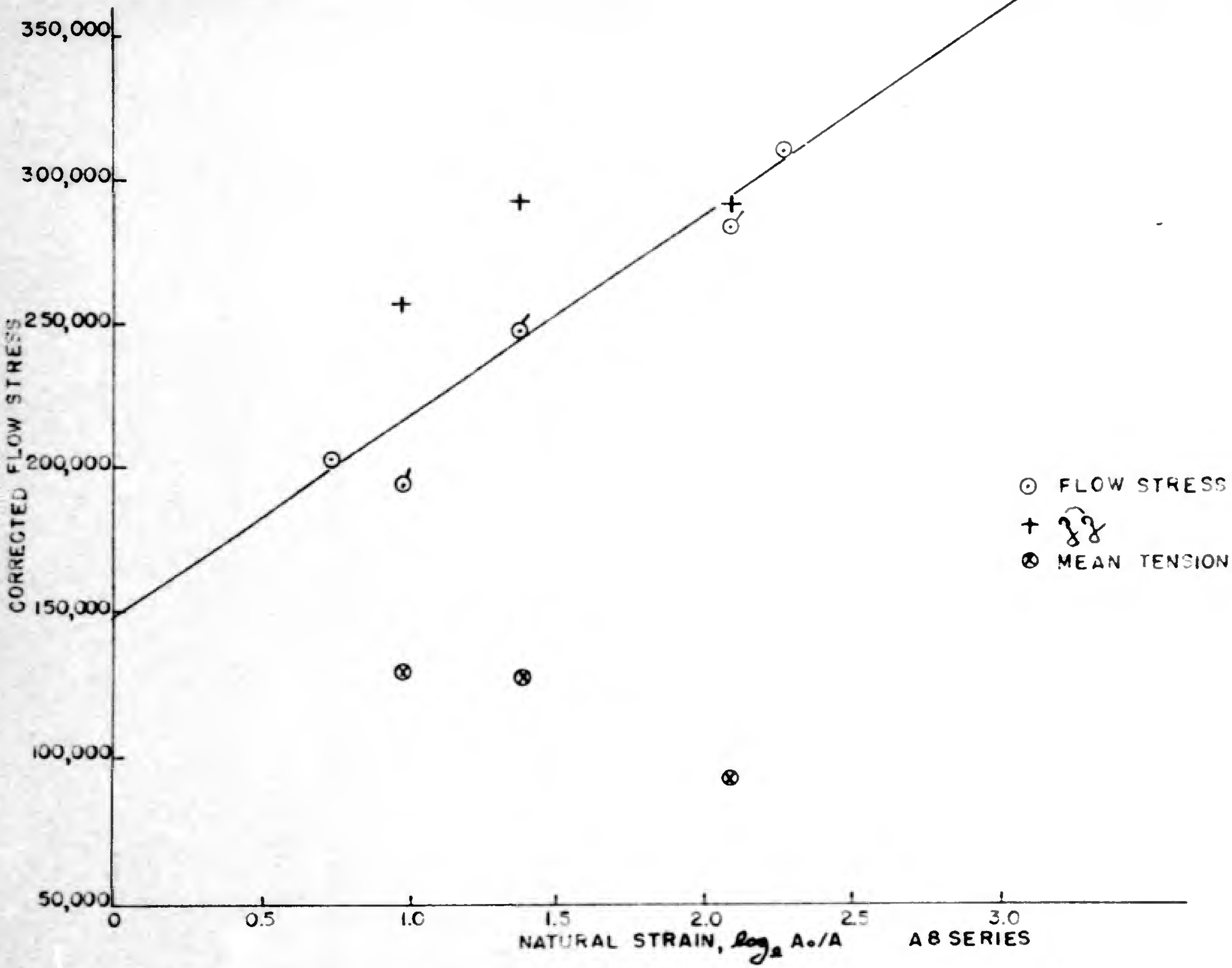

350,000
300,000
250,000
200,000
150,000
100,000
50,000
CORRECTED FLOW STRESS
0
0.5
1.0
1.5
2.0
2.5
3.0
NATURAL STRAIN, $\log_e A_o/A$
A8 SERIES
FLOW STRESS
MEAN TENSION

FIG. 9

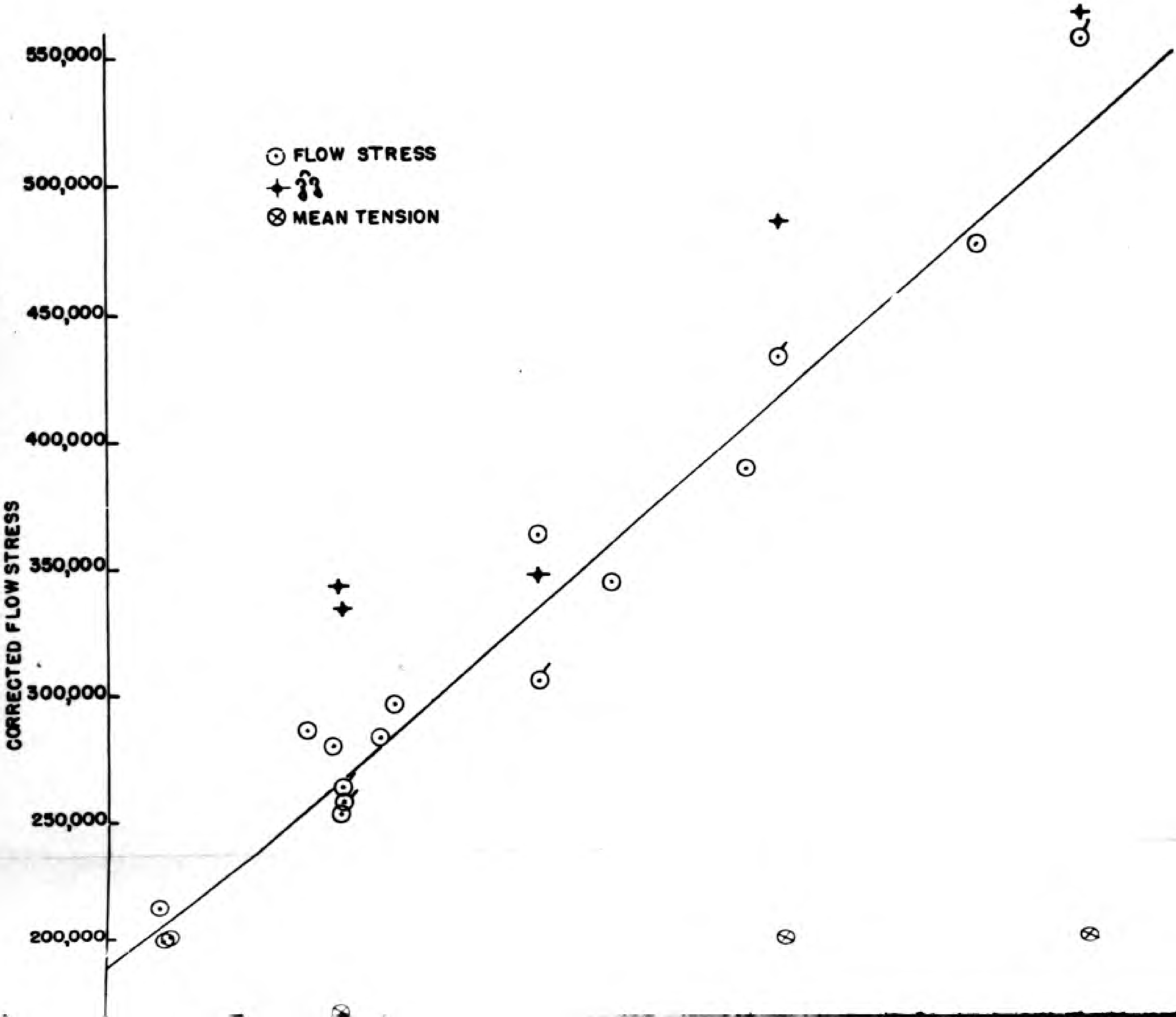

550,000
500,000
450,000
400,000
350,000
300,000
250,000
200,000
CORRECTED FLOW STRESS
FLOW STRESS
MEAN TENSION

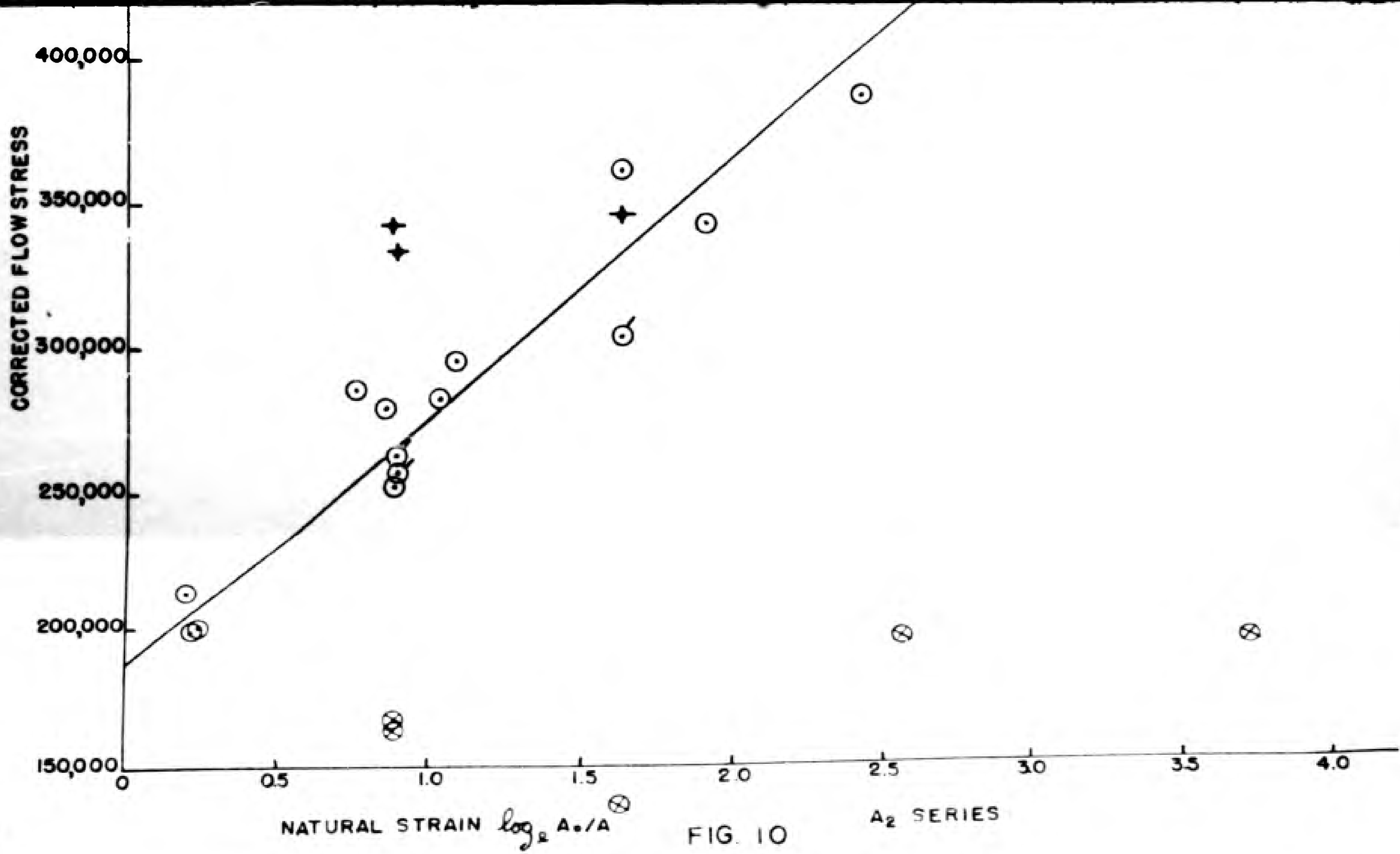
CORRECTED FLOW STRESS
400,000
350,000
300,000
250,000
200,000
150,000
0
0.5
1.0
1.5
2.0
2.5
3.0
3.5
4.0
NATURAL STRAIN $\log_e A_0/A$
A_2 SERIES

FIG. 10

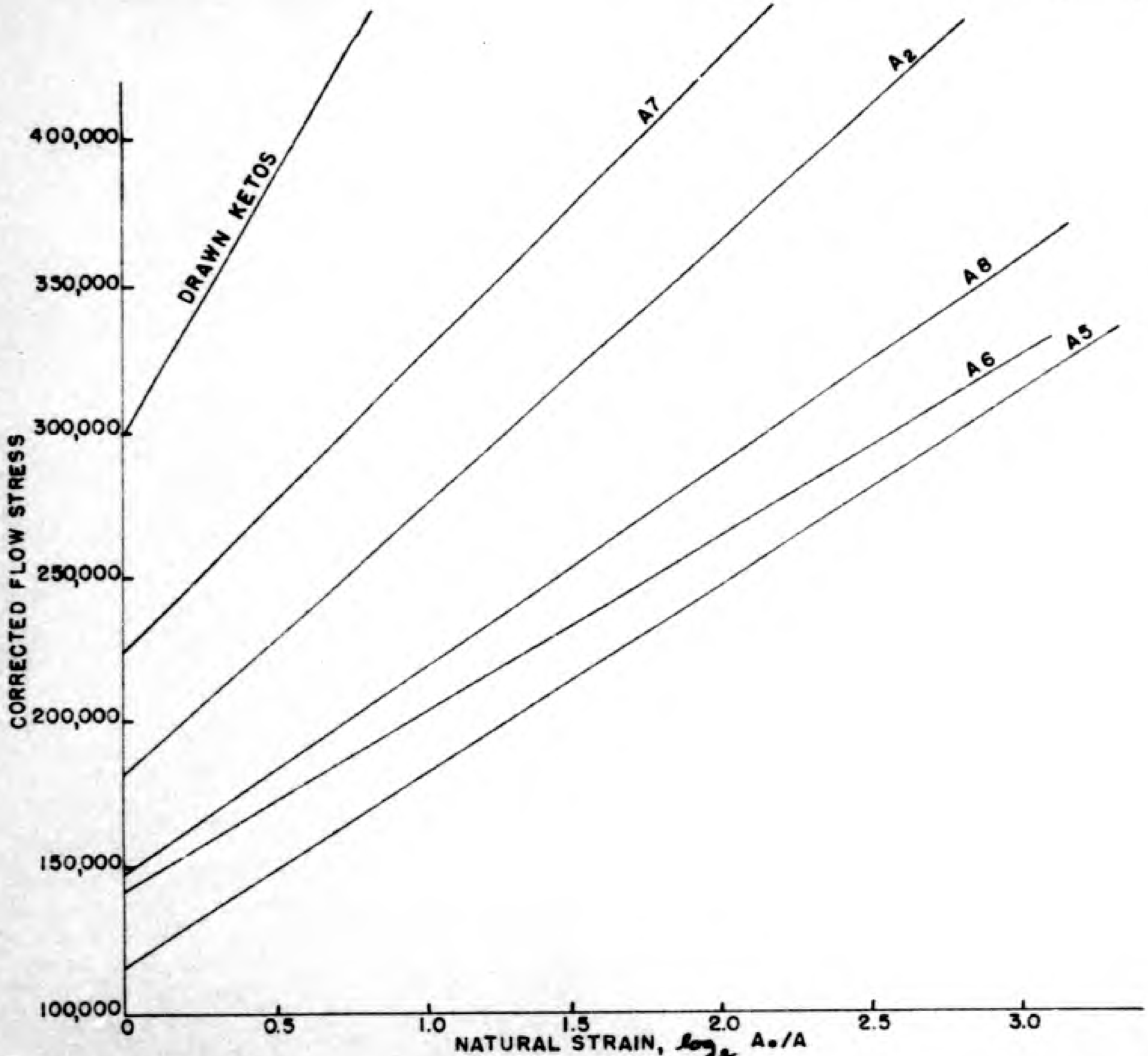
DRAWN KETOS
A7
A2
A8
A6
A5
400,000
350,000
300,000
250,000
200,000
150,000
100,000
CORRECTED FLOW STRESS
0
0.5
1.0
1.5
2.0
2.5
3.0
NATURAL STRAIN, loge A₀/A

FIG. 11

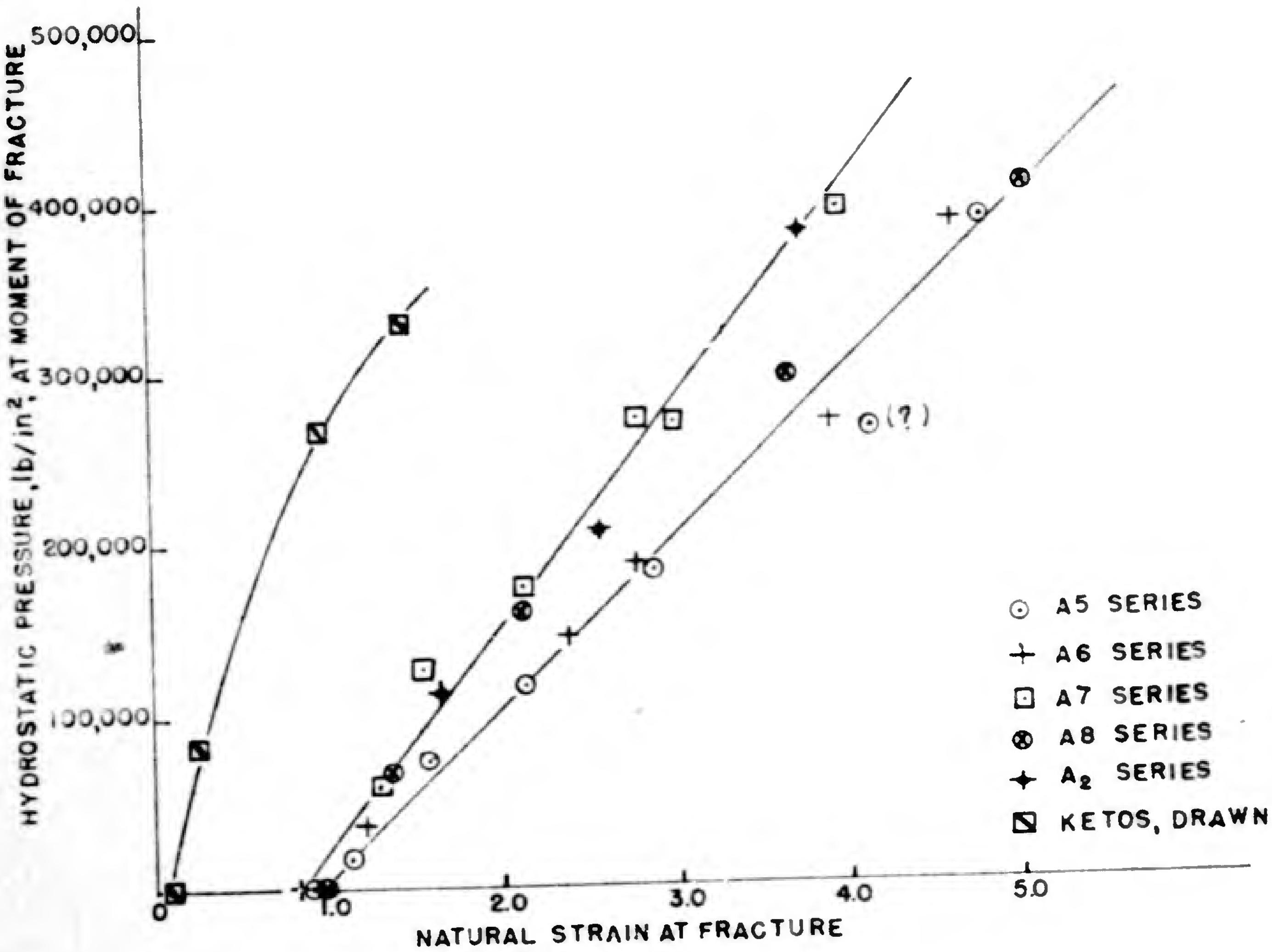
HYDROSTATIC PRESSURE, lb/in², AT MOMENT OF FRACTURE
500,000
400,000
300,000
200,000
100,000
0
1.0
2.0
3.0
4.0
5.0
NATURAL STRAIN AT FRACTURE
(?)
A5 SERIES
A6 SERIES
A7 SERIES
A8 SERIES
A2 SERIES
KETOS, DRAWN

FIG. 12

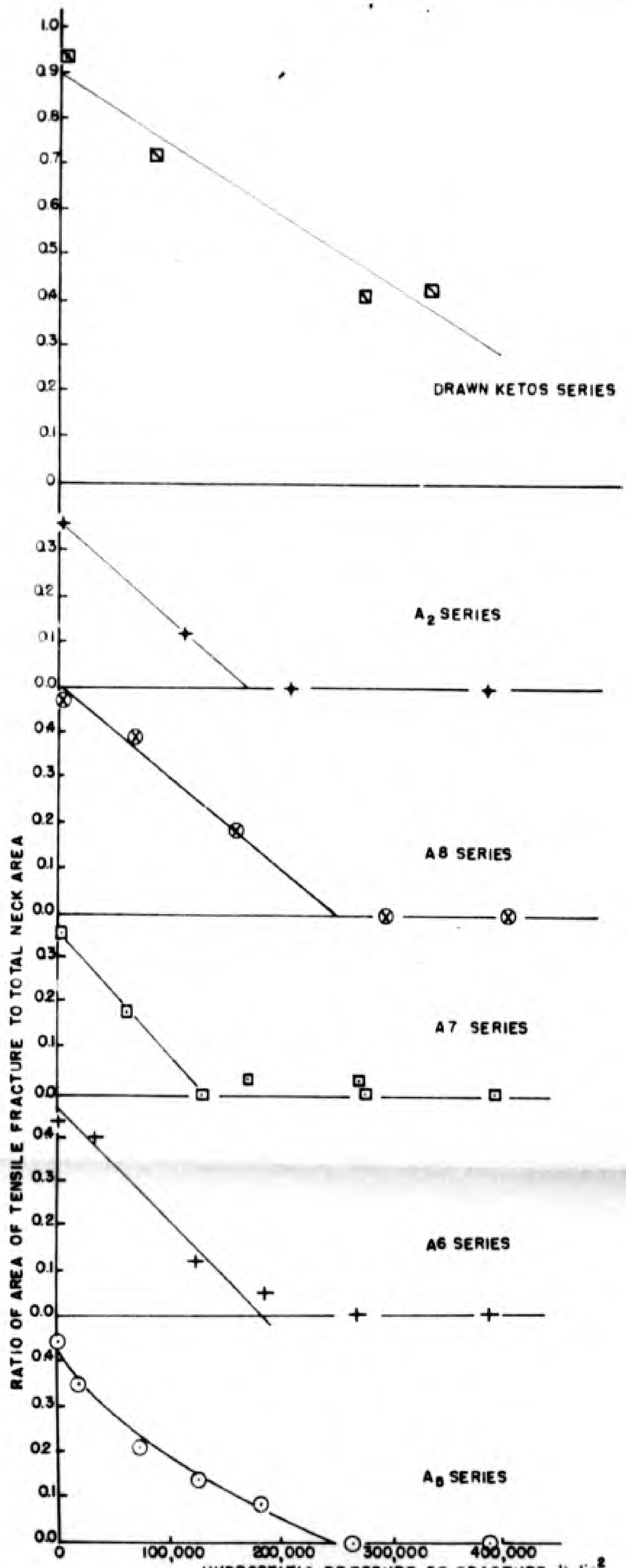
DRAWN KETOS SERIES
A_2 SERIES
A8 SERIES
A7 SERIES
A6 SERIES
A_8 SERIES
RATIO OF AREA OF TENSILE FRACTURE TO TOTAL NECK AREA
HYDROSTATIC PRESSURE OF FRACTURE, lb/in²
0
100,000
200,000
300,000
400,000

FIG. 13

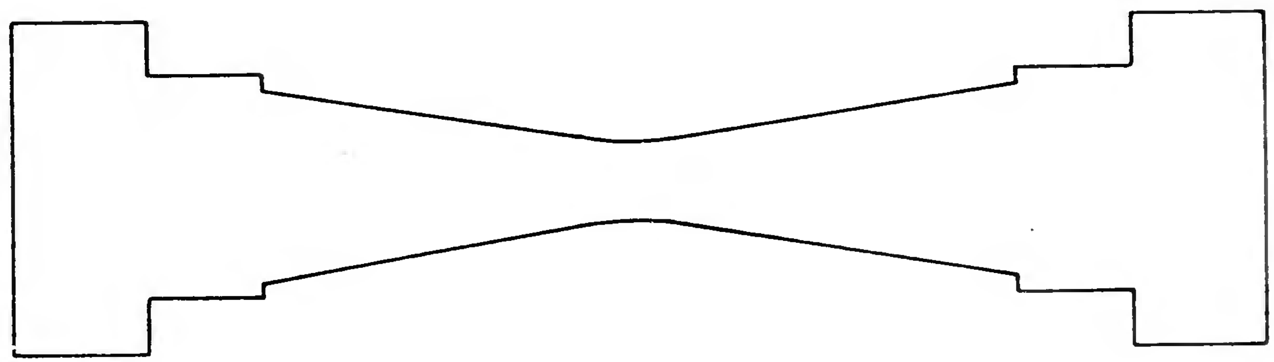

FIG. 14
REFIGURED TENSION SPECIMEN

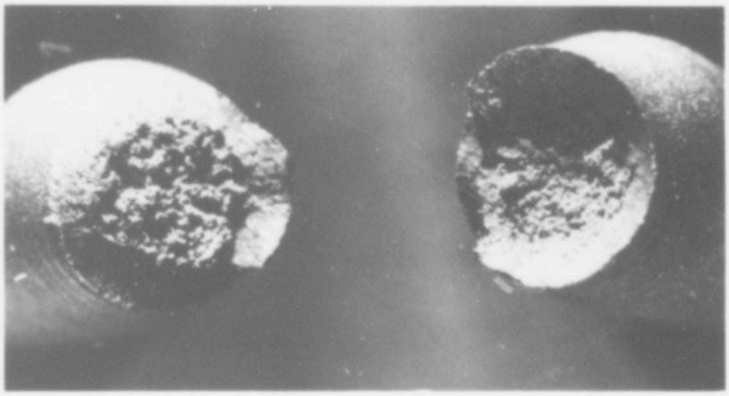

Fig. 15
Broken at Atmospheric Pressure (A6-A7)
X 10

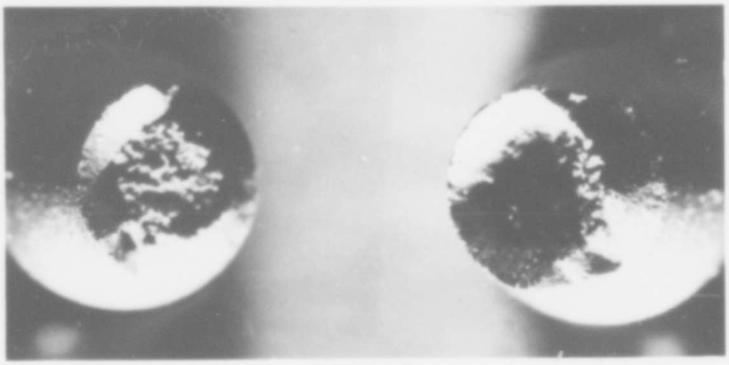

Fig. 16
Broken under 34,000 psi (A6-A5)
X 10

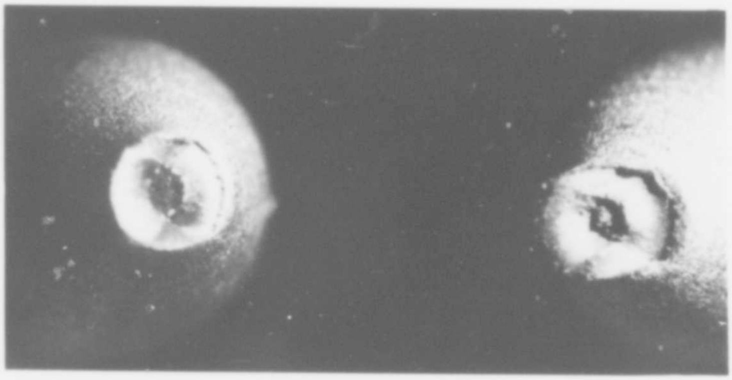

Fig. 17
Broken under 145,000 psi (A6-A3)
X 12

WTN.639-6012

EXAMPLES OF CUP-CONE TYPE OF FRACTURE, SHOWING NON-FITTING OF SURFACES

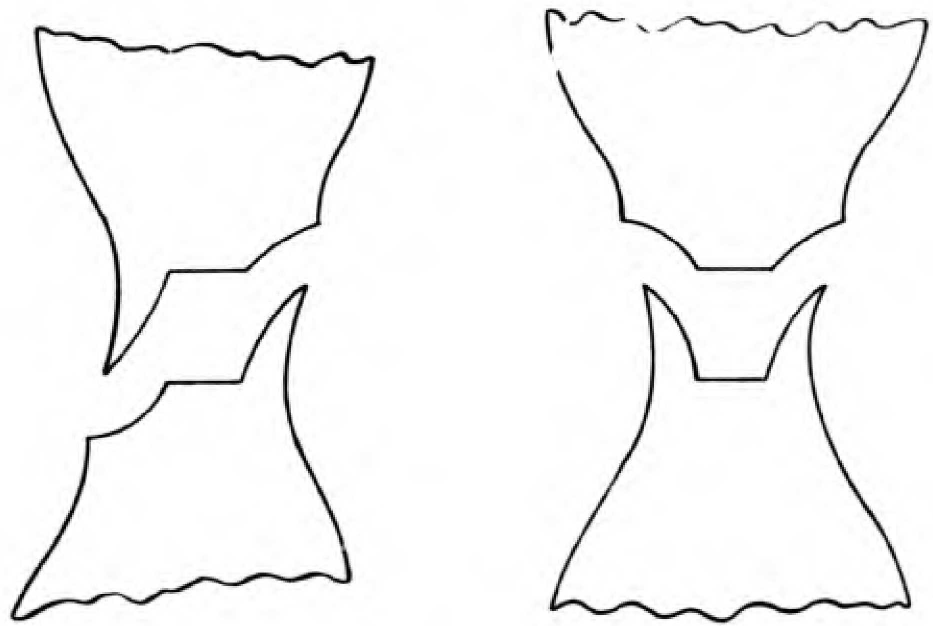

FIG. 21

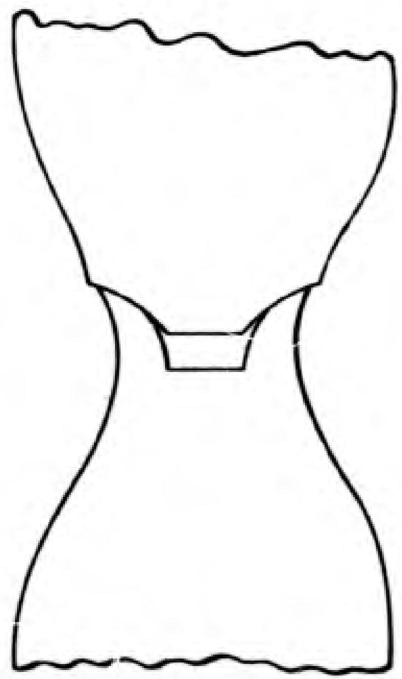

FIG. 22
HYPOTHETICAL INTERMEDIATE
STAGE OF FRACTURE

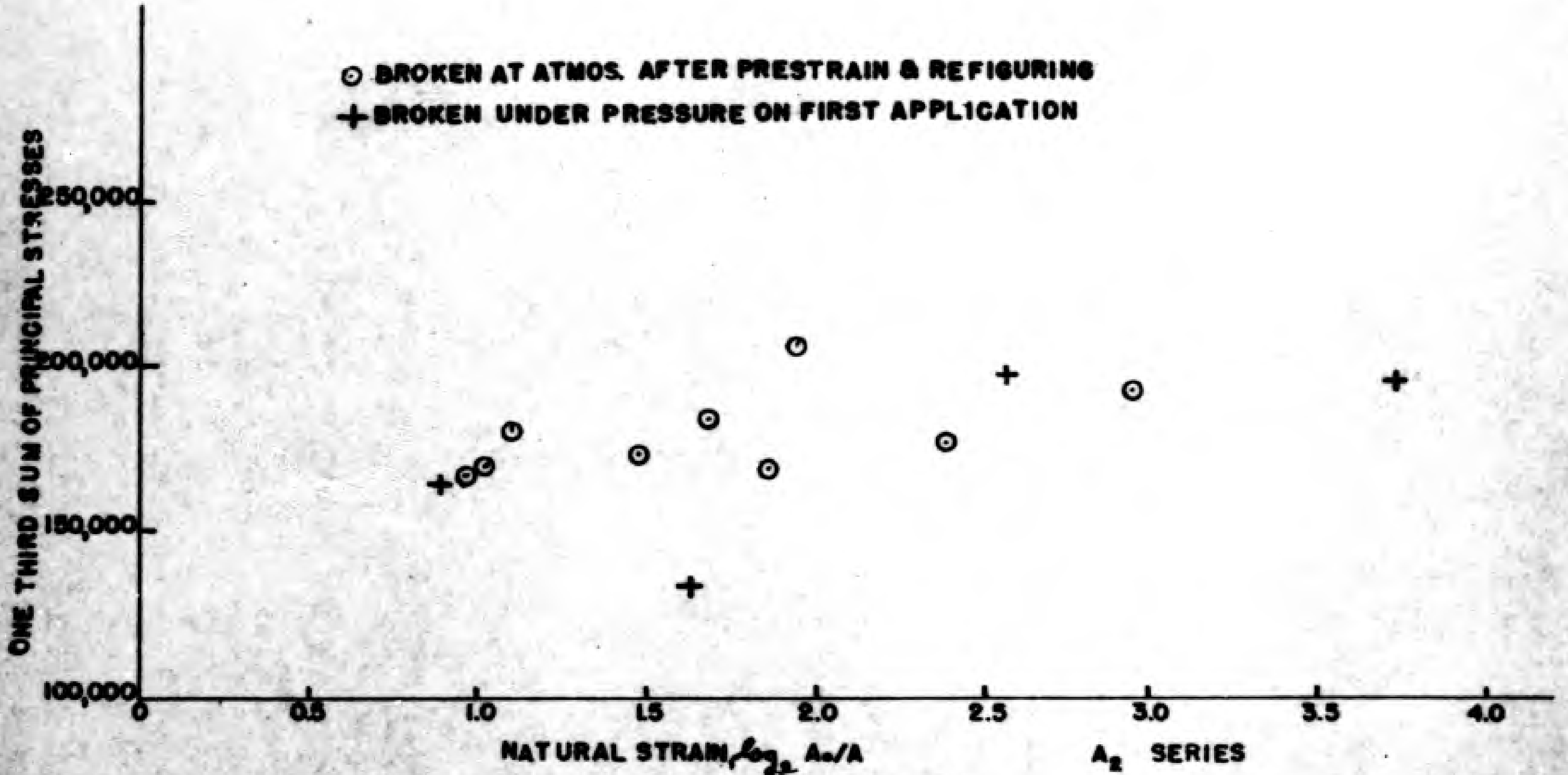
⊙ BROKEN AT ATMOS. AFTER PRESTRAIN & REFIGURING
+ BROKEN UNDER PRESSURE ON FIRST APPLICATION
ONE THIRD SUM OF PRINCIPAL STRESSES
250,000
200,000
150,000
100,000
0
0.5
1.0
1.5
2.0
2.5
3.0
3.5
4.0
NATURAL STRAIN, $\log_e A_0/A$
A_2 SERIES

FIG. 23